OUKA
Osaka University Knowledge Archive

Title	希土類系水素吸蔵合金薄膜に関する研究
Author(s)	坂口, 裕樹
Citation	大阪大学, 1988, 博士論文
Version Type	VoR
URL	https://hdl.handle.net/11094/2760
rights	
Note	

Osaka University Knowledge Archive : OUKA

https://ir.library.osaka-u.ac.jp/

Osaka University

STUDIES ON RARE-EARTH HYDROGEN STORAGE ALLOY FILMS

HIROKI SAKAGUCHI

1988

STUDIES ON RARE-EARTH HYDROGEN STORAGE ALLOY FILMS

(希土類系水素吸蔵合金薄膜に関する研究)

HIROKI SAKAGUCHI

1988

PREFACE

The work described in this thesis was carried out under the guidance from Professors Jiro Shiokawa and Hiroshi Yoneyama at the Department of Applied Chemistry, Faculty of Engineering, Osaka University.

The object of this thesis is to study the mechanical and electrical properties of the rare-earth hydrogen storage alloy films. Furthermore, the development of a new method of hydrogen separation is tried using the films.

Hiroki Sakaguchi

Suita, Osaka

January, 1988

CONTENTS

Chapter 1

GENERAL INTRODUCTION

Extensive studies have been put in practice on the $LaNi_5$ family of hydrogen storage intermetallic compounds. Excellent properties of the materials to take up a large amount of hydrogen quickly and reversibly under moderate conditions have proposed their use in a lot of applications such as heat pumps, hydrogen purification and batteries[1-6].

A serious drawback regarding the practical use of $LaNi_5$ is the fact that the material pulverizes during hydrogen charging[7,8]. The volume increase associated with the formation of the hydrides leads to stresses in the hydride envelope on the unhydride core material. This stress causes cracks which pulverize the hydride[9]. For $LaNi_5$ subjected to several charging-decharging cycles, the particle diameter was measured to be about 10 μm, though there was a broad distribution in size[10,11].

An amorphous alloy which is prepared by rapid cooling is known to have a considerable resistance to a stress since a strain can be relaxed by the free volume existing in an alloy. The amorphous alloy is, therefore, a promising material for hydrogen storage.

Some thin films of $LaNi_5$ which were obtained by using a flash-evaporation method were amorphous and did not pulverize after repeated the hydrogen absorption-desorption cycling. An investigation of electrical properties of the films has

been performed[12,13].

In this study, thin films of hydrogen storage alloys were prepared, and properties of the films, such as electrical properties and hydrogen content in the films, were investigated. Furthermore, the development of a new method of hydrogen separation was tried using the films.

The technological development for the hydrogen storage materials has been performed in connection with energy storage or heat pumps. Another valuable usage, however, should be considered because there are problems with respect to the weight and the cost owing to the use of enormous volumes of metal. A new usage of hydrogen storage materials is introduced in this study.

General introduction is presented in chapter 1.

In chapter 2, preparation of thin films of $LaNi_5$, $SmCo_5$ and $LaCo_5$ using a flash-evaporation method as well as a sputtering method is described. The reason for taking $SmCo_5$ is that $SmCo_5$ is a strong magnet and $LaCo_5$ is because its volume expansivity at hydrogen absorption is a half of the $LaNi_5$ equivalent.

In chapter 3, the dulability of the $LaNi_5$ films formed on various substrates against the hydrogen absorption-desorption process, the adherenceness of the film to various substrates and the abrasion-resistant properties are to be discussed.

In chapter 4, effects of hydrogen absorption on electrical resistivities of the films are studied and the mechanism of hydrogen absorption-desorption is considered.

In chapter 5, the hydrogen content in the films is de-

scribed based on a quartz-crystal mass-monitoring method.

In chapter 6, the hydrogen permeability of various metals are examined by observing the development of color of amorphous WO_3 with hydrogen permeated through metal films on which an $LaNi_5$ film was coated.

In chapter 7, hydrogen separation using $LaNi_5$ films are discussed.

In chapter 8, concluding remarks are presented.

The contents of this thesis are composed of the following papers.

(1) Measurements of Hydrogen Contents in $LaNi_5$ Films
H. Sakaguchi, K. Niki, H. Nagai, G. Adachi and J. Shiokawa
Denki Kagaku, 52(10)(1984)706.

(2) The Effect of Hydrogen Absorption on the Electrical Resistivities of $SmCo_5$ and $LaNi_5$ Films
H. Sakaguchi, H. Nagai, G. Adachi and J. Shiokawa
J. Mat. Sci. Lett., 4(1985)347.

(3) Preparation of $LaNi_5$ Films and Effects of Hydrogen Absorption on Electrical Resistivities of the Films
G. Adachi, H. Sakaguchi, K. Niki, H. Nagai and J. Shiokawa
Bull. Chem. Soc. Jpn., 58(1985)885.

(4) Determination of the Hydrogen Content in Amorphous $LaNi_5$ Films Using a Quartz-Crystal Mass-Monitoring Method
H. Sakaguchi, N. Taniguchi, N. Nagai, K. Niki, G. Adachi and J. Shiokawa
J. Phys. Chem., 89(1985)5550.

(5) Colouring of Amorphous WO_3 with Hydrogen Penetrated through an $LaNi_5$ Thin Film

G. Adachi, H. Sakaguchi, T. Shimogohri and J. Shiokawa

J. Less-Common Met., 116(1986)L13.

(6) Preparation of $LaNi_5$ Films on an Aluminum or a Copper Foil Substrate

H. Sakaguchi, G. Adachi and J. Shiokawa

J. Less-Common Met., 118(1986)L1.

(7) Hydrogen Separation Using $LaNi_5$ Films

H. Sakaguchi, H. Nagai, G. Adachi and J. Shiokawa

J. Less-Common Met., 126(1986)83.

(8) Studies on Hydrogen Permeability for Various Metals Using the Coloring of Amorphous WO_3 with Hydrogen Penetrated through Sandwich-Type Films(a-WO_3/Metal /$LaNi_5$)

G. Adachi, H. Sakaguchi, T. Shimogohri and J. Shiokawa

J. Less-Common Met., 133(1987)271.

(9) Effects of Hydrogen Absorption on the Electric Resistivity of $LaCo_5$ Films and Determination of the Hydrogen Content in the Films

H. Sakaguchi, Y. Yagi, N. Taniguchi, G. Adachi and J. Shiokawa

J. Less-Common Met., 135(1987)137.

(10) Characterization of $LaNi_5$ Thin Films Prepared by Sputtering and Evaporating Methods

H. Sakaguchi, N. Taniguchi, H. Seri, G. Adachi and J. Shiokawa

Nippon Kagaku Kaishi, (1987)1875.

(11) Hydrogen Separation Using $LaNi_5$ Films Deposited on Polymer Membranes

H. Sakaguchi, G. Adachi and J. Shiokawa

Bull. Chem. Soc. Jpn., in press.

Chapter 2

PREPARATION OF HYDROGEN STORAGE ALLOY FILMS BY MEANS OF VAPOR DEPOSITION AND SPUTTERING METHODS, AND CHARACTERIZATION OF THE FILMS

2. 1. Introduction

The preparation of a thin film of an alloy by means of a conventional thermal evaporating method is difficult owing to the difference in the vapor pressure of component metals.

Thin films of $LaNi_5$, $SmCo_5$ and $LaCo_5$ were prepared using a flash evaporation-deposition method that component metals can be vaporized quickly and completely. A sputtering method was also used to prepare thin films of $LaNi_5$. The films obtained were characterized with analyses of composition and crystal structure, and the measurement of density.

2. 2. Experimental

2. 2. 1. Preparation of films

Deposited films. $LaNi_5$ (La 32.16, Ni 67.84 wt%) powder was supplied by Santoku Metal Industry Co. Ltd., Kobe. The $LaNi_5$ powder was placed on a tungsten boat which was preheated up to a temperature of 2.3×10^3 K. Both components

of $LaNi_5$ evaporated immediately (at this temperature) and were deposited onto a substrate which was placed just above the tungsten boat. The alloy powder was supplied by a conveyor belt equipped with a hopper. The vacuum during deposition was ca. 10^{-3} Pa. After deposition, pure helium gas was allowed into the chamber to prevent the formation of an oxide on the films.

Sputtered films. The preparation of sputtered films was performed with an r.f. magnetron sputtering apparatus made by Daia Vacuum Engineering Co., Ltd., from an $LaNi_5$ target[14,15]. The r.f. generating power applied was 400 W and the substrate temperatures were in the range of 300-373 K. The atmosphere used for the discharge was 99.99 % purity argon at a pressure of 0.395 Pa.

2. 2. 2. Characterization of films

The instruments for evaluation were as follows : a Rigaku X-ray powder diffractometer for structural characterization, a Rigaku X-ray energy spectrometer for the determination of composition, a Shimadzu ESCA 650B electron spectrometer for the depth profile observation of chemical composition. The thickness of the films obtained was determined by direct observation of the cross section of the samples using a Hitachi S-405 scanning electron microscope.

The density of the films deposited on the quartz crystal sheet(Eiko Inc.) and the copper sheet(99.5 % pure, 0.3 mm thick, The Japan Lamp Ind., Co., Ltd.)

was obtained by the calculation from their weight, area and thickness.

The hardness of the films deposited on the glass sheet(micro slide glass, 1 mm thick, Matsunami Glass Ind., Ltd.) was measured by means of a Shimadzu dynamic ultra-microhardness tester(DUH-50).

The thermal conductivity measurements were performed using a Sinku-Riko thermal constant analyzer by a.c. calorimetric method(PIT-1). The substrate used was a Teflon sheet(10 mm long, 4 mm wide and 5 nm thick, supplied by Japan Asbestos Inc.) which had been cleaned in an ultrasonic washing machine filled with acetone. The thermal conductivity(k) of the deposited film is given by

$$k = Q_1(D_1-D_2)t_2/t_1$$

where Q_1 is the heat capacity of the $LaNi_5$ deposited Teflon sheet, D_1 and D_2 are the thermal diffusivity of the $LaNi_5$ coating the Teflon sheet and that of the teflon sheet, respectively, t_1 and t_2 are thickness of the $LaNi_5$ film and that of the Teflon sheet, respectively.

2. 3. Results and Discussion

2. 3. 1. Characterization of the $LaNi_5$ films

The chemical composition of the films determined by means of the X-ray fluorescence method was the same as that of the original $LaNi_5$ and variation of the composition due to the difference of thickness was not ob-

served. As the result of a X-ray photoelectron spectroscopy measurement, it was found that the surface of the films was coated with a oxide layer with a thickness of about $2x10^{-2}$ μm for deposited films and below $1x10^{-2}$ μm for sputtered films, and the composition of the inner parts of the films was homogeneous.

Figure 1 shows the X-ray diffraction data for a crystalline sample and $LaNi_5$ films. Diffraction patterns of a sputtered film and a deposited film exhibited a broad band characteristic of an amorphous material. However, for the sputtered film, the crystalline peaks still remained though the intensity of the peaks is weak.

Table 1 shows density, thermal conductivity and hardness for both the sputtered film and the deposited film. The density of the sputtered film was about 6 gcm^{-3} which was found to be smaller than that of the crystalline sample[16] and was larger than that of the deposited film[17].

The thermal conductivities of the films were 2.16 $Wm^{-1}K^{-1}$ for the sputtered film and 2.43 $Wm^{-1}K^{-1}$ for the deposited film. There was no significant difference between them.

As for the hardness measurement, a glass substrate had to be used because the hardness of the metal such as Cu or Ni is smaller than that of the $LaNi_5$ film. The hardness of the sputtered film was larger than that of the deposited film, because the density and the crystallinity of the sputtered film are larger than those

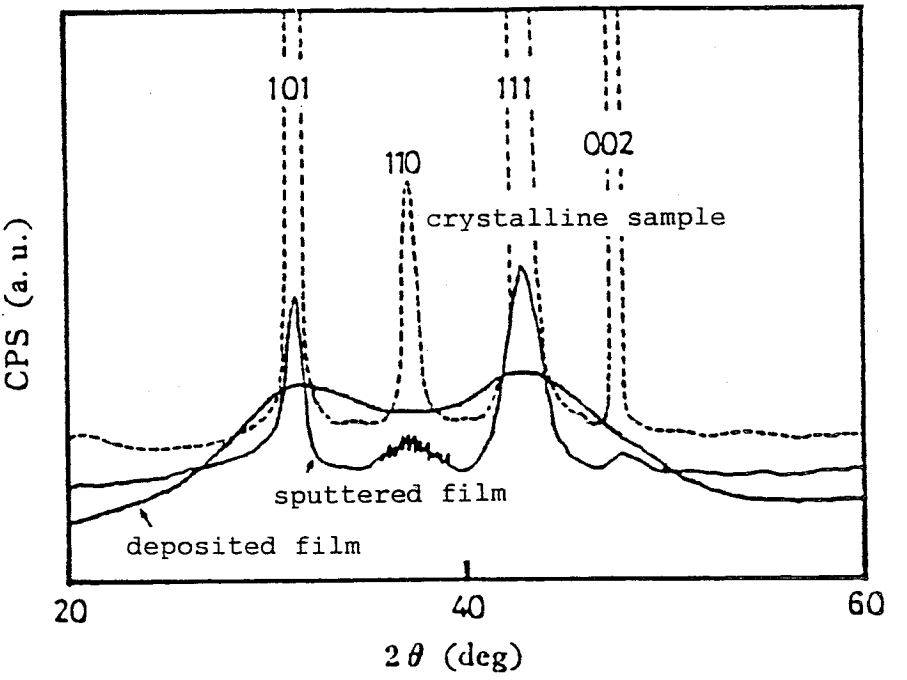

Fig. 1 X-ray diffraction patterns.

Table 1 Characterization of $LaNi_5$ films

	Bulk	Sputtered film	Deposited film
Density (g/cm^3)	8.3	6	4
Thermal conductivity (W/m·k)	1.32	2.16	2.43
Hardness	—	503	349

of the deposited film.

The surface of the sputtered films was found to be smooth and dense compared with the deposited film.

2. 3. 2. Characterization of $SmCo_5$ and $LaCo_5$ films

The chemical composition of the La-Co films was the same as that of the original $LaCo_5$. For the Sm-Co film, the composition was $SmCo_{3.5}$ because the vapor pressure of samarium is much larger than that of cobalt. An $SmCo_5$ film was obtained by the addition of 3 wt% cobalt to the raw material.

Obtained films were amorphous, at least as determined from X-ray diffraction results.

2. 4. Summary

Thin films of $LaNi_5$, $SmCo_5$ and $LaCo_5$ were prepared by means of flash evaporation-deposition and sputtering techniques. The films obtained were amorphous. The density of the sputtered $LaNi_5$ film, i.e. 6 gcm^{-3}, was larger than that of the deposited film or smaller than that of a crystalline sample. Thermal conductivities of the films were larger than those of a bulk sample. The surface of the sputtered films was found to be smooth and dense compared with the deposited films.

Chapter 3

MECHANICAL PROPERTIES OF $LaNi_5$ THIN FILMS PREPARED BY VAPOR DEPOSITION AND SPUTTERING METHODS

3. 1. Introduction

Rare-earth hydrogen storage alloys pulverizes after repeated hydrogen absorption-desorption cycle due to a large cubic expansivity at the hydrogenation, e.g. 25 % for $LaNi_5$. The pulverization is a serious problem for the technical use of the materials because of the scattering of the powder of alloy in the vessel, a lowering of the heat transfer efficiency and the ocurrence of the local stress.

In the present study, the dulability of the $LaNi_5$ films formed on various substrates against the hydrogen absorption-desorption process, the adherenceness of the film to various substrates and the abrasion-resistant properties were investigated.

3. 2. Experimental

Deposited films. The substrates were aluminum(55 mm x 100 mm x 15 μm, 99.3 wt.% Al) and copper (50 mm x 95 mm x 20 μm, 99.5 wt.% Cu) foils. These were washed first with acetone and

then with methanol. $LaNi_5$ was deposited on them by the flash evaporation. A distance between tungsten boat and the substrate was 40 mm and the substrate temperature during the evaporation was about 600 K. The samples put into a pressure vessel and at 363 K, a pressure of 2.5×10^6 Pa of hydrogen was applied for 15 min, then the system was evacuated for 15 min. The process repeated 75 times. An appearence of the films was examined with the naked eye and an optical microscope.

Sputtered films. The dulability of the films formed on various substrates against the hydrogen absorption-desorption process was determined as follows. Substrates used were a glass sheet(micro slide glass, 1 mm thick, Matsunami Glass Ind., Ltd.), an aluminum sheet(99.5 % pure, 0.3 mm thick, The Japan Lamp Ind., Co., Ltd.), a copper sheet (the purity, the thickness and the manufacture are the same as the aluminum sheet), a nickel sheet (the purity, the thickness and the manufacture are also the same as the aluminum sheet), an aluminum foil(99.5 % pure, 15 μm thick, Toyo Aluminum Inc.), a copper foil (99.5 % pure, 20 μm thick, The Japan Lamp Ind., Co., Ltd.) and a nickel foil (the purity, the thickness and the manufacture are also the same as the copper foil). After cleaning in an ultrasonic washing machine filled with acetone, these substrates were coated with the $LaNi_5$ films with a thickness of 2.1 μm or 4.3 μm. The measurement was the same as that of the deposited films. However, the time during the charging or discharging of hydrogen was 10 min, and the process repeated 100 times.

3. 2. 2. Adherenceness of the $LaNi_5$ film to various substrates

The adherenceness of the $LaNi_5$ film to various substrates and the abrasion-resistant properties were investigated with a pencil hardness test[18], a peel test[19] and a rubbing test[19]. The pencil hardness test consists of an operator moving a pencil of known hardness at a 45-deg angle across the surface of the film with just enough pressure to hold the pencil securely. The pencil hardness of the film is reported as the hardest pencil that does not scratch or gouge the surface of the film. The peel test is that an adhesive tape is pressed onto the film and then torn off; the adhesion is classified according to whether the film is wholly or partially removed from the substrate with the tape or not removed at all. The abrasion test is that the film is rubbed with various rubbers having the different hardness.

3. 3. Results and Discussion

Deposited films. Figure 1 shows an optical micrograph of the surface of an $LaNi_5$ film(10.5 μm thick) on aluminum as a substrate after testing. In spite of testing for 75 cycles, the $LaNi_5$ film has not been pulverized at all. As is shown in Fig. 2, the similar result was obtained for a copper foil, on which $LaNi_5$ was deposited(12.5 μm thick).

The reason why the $LaNi_5$ film has not been disintegrated seems to be that the structure of the film is amorphous and

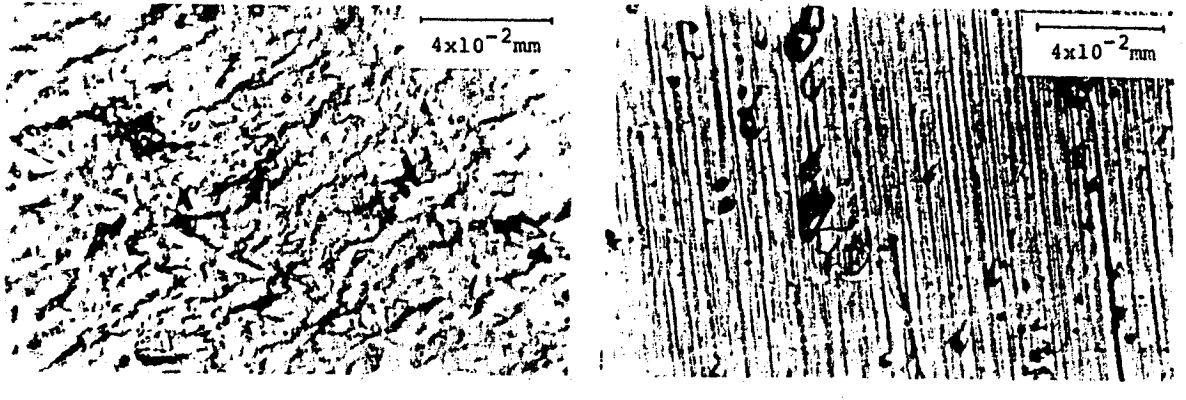

Fig. 1 An optical micrograph of the surface of an $LaNi_5$ film on an aluminum foil after testing.

Fig. 2 An optical micrograph of the surface of an $LaNi_5$ film on a copper foil after testing.

the amount of hydrogen taken up by the film is relatively small[17].

The thermal conductivity of the $LaNi_5$ hydride powder is very poor because the area of contact among the particles is small. For the samples obtained, in which the $LaNi_5$ film and the metal foil are in close contact, it seems that the thermal conductivity will be remarkably high.

The strong high thermal conductivity $LaNi_5$ film is suitable for application to use as a heat pump and for hydrogen separation.

Sputtered films. Table 1 shows the durability of the sputtered $LaNi_5$ film against the cycle of the hydrogen absorption-desorption process. A film with a thickness of below 0.5 μm deposited on the quartz crystal sheet has not been disintegrated after repeated hydrogenation-dehydrogenation cycle(100 cycles). It was confirmed that the films coated on the glass, the aluminum sheet or the copper sheet had already exfoliated at the tenth cycle. It was found that the thicker film is easy to disintegrate. The durability of the film deposited on the foil was larger than that of the film deposited on the sheet for the same metal substrate.

Table 2 reveals results of the adhesion tests for the $LaNi_5$ sputtered film deposited on various substrates after 100 cycles of hydrogen absorption-desorption process. For the 2.1 μm thick film, the film on the glass sheet and the aluminum sheet had been peeled easily.

The degree of the exfoliation for the glass substrate was larger than that for the aluminum substrate. For the

Table 1 Mechanical strength of sputtered films for hydrogen absorption-desorption cycles

Thickness of film (μm)	Substrate	Substrate thickness (μm)	The number of cycling									
			10th	20th	30th	40th	50th	60th	70th	80th	90th	100th
2.1	Glass	1000	x	x	x	x	x	x	x	x	x	x
	Al	300	x	x	x	x	x	x	x	x	x	x
	Ni	300										
	Cu	300							△	△	△	△
	Al foil	15										
	Ni foil	20										
	Cu foil	20										
4.3	Ni	300										
	Cu	300	x	x	x	x	x	x	x	x	x	x
	Al foil	15										
	Ni foil	20										
	Cu foil	20	△	x	x	x	x	x	x	x	x	x

△ : Subtle exfoliation was observed.
x : Obvious exfoliation was observed.

Table 2 Adhesion of sputtered films deposited on various substrates

Thickness of film (μm)	Substrate	thickness (μm)	Mechanical* strength test 3B	F	2H	4H	Exfoliation test	Abrasion-resistance test** Plastic	Rubber	Rotring	Sand
2.1	Glass	1000		△	x	x	x				△
	Al	300			△	x	x		△	x	x
	Ni	300									△
	Cu	300				△					△
	Al foil	15									△
	Ni foil	20									△
	Cu foil	20									△
4.3	Ni	300									
	Cu	300			△	△	x				△
	Al foil	15									△
	Ni foil	20									
	Cu foil	20				x	x	△	△	△	x

△ : Flaw x : Exfoliation

x : Exfoliation

△ : Subtle abrasion was observed.

x : Obvious abrasion was observed.

* The film is scratched with pencils of various hardness.
Notation indicates hardness of the pencils used.

**The film is rubbed with eraseres of various hardness.
The order of hardness ; Plastic<Rubber<Rotring<Sand.

thicker film, the exfoliation was observed even for the films deposited on the copper sheet and the copper foil.

The adhesion between the sputtered $LaNi_5$ film and the substrate was in the following order for the substrates used, Ni foil>Ni>Al foil>Cu foil>Cu>Al>Glass.

The order of the adhesiveness appears to be due to the difference of the thermal expansivity between the film and the substrate. The thermal expansivity of substrates is in the following order, $Al(2.55\times10^{-5}\ K^{-1})>Cu(1.75\times10^{-5})>Ni(1.65\times10^{-5})>>Glass(3.68\times10^{-6})$[20]. The thermal expansivity of $LaNi_5$ has not been obtained. However, since the thermal expansivity of $LaNi_5$ seems to be the same as that of nickel, the bonding between the two was strong. The adhesion became weak according to the increase in the difference of the thermal expansivity between the $LaNi_5$ film and substrate metals. The thermal expansivity of the glass is extremely low in comparison with $LaNi_5$, so that the exfoliation appeared to occur easily.

From the analogous point of view, it is noticed that the ductility, especialy lengthening of the substrate materials is in the following order Al>Cu>Ni[21]. Since nickel has almost the same ductility as $LaNi_5$, the adhesion was superior to others.

The adhesion of the thicker $LaNi_5$ films was inferior to that of the thinner one, because the strain due to the internal stress caused by the deposition of the film increases with thickness.

The degree of disintegration of the film deposited

on the foil was smaller than that on the sheet for the same metal substrates owing to that the stress relief occurs due to the plastic deformation when the stress is applied to the foil, while for the sheet the stress applied is repelled to the film because of the elastic deformation.

The adhesion between the film and the metal substrate was stronger than that between the film and the glass substrate owing to the surface condition of the metal, i.e. an anchor effect.

3. 4. Summary

The dulability of the films obtained against the hydrogen absorption-desorption was found to be very large in comparison with a bulk sample. The bonding between the $LaNi_5$ films and nickel substrates was extremely strong because the thermal expansivity of $LaNi_5$ seems to be the same as that of nickel.

Chapter 4

MECHANISM OF HYDROGEN ABSORPTION-DESORPTION (EFFECTS OF HYDROGEN ABSORPTION ON ELECTRICAL RESISTIVITIES OF RARE-EARTH HYDROGEN STORAGE ALLOY FILMS)

4. 1. Introduction

It was found that thin films of rare-earth hydrogen storage alloys had not been pulverized during the hydrogen absorption-desorption cycle. Therefore, it has been possible to measure the electrical resistivity using these films.

The objects of this study were to reveal the mechanism of hydrogen absorption-desorption through the electrical properties of the films.

4. 2. Experimental

Films of $LaNi_5$, $SmCo_5$ and $LaCo_5$ were prepared using a flash evaporation-deposition method.

Quartz plates used as a substrate were first soaked in a HCl-HNO_3 mixed solution for 1 day and were then washed with a neutral detergent and rinsed with de-ionized water. The plate was cleaned with an ultrasonic washing machine filled with

de-ionized water before drying in a desiccator.

An apparatus used for measuring electrical resistivities is shown in Fig. 1. A sample was installed in the apparatus which was made of 316 stainless steel. The vessel was connected to a high pressure manifold with connections to a vacuum pump and a high pressure hydrogen gas(99.99 % purity) cylinder.

The resistivity was measured by means of a four-probe d.c. technique. The voltage drop across the film at a constant current was recorded as a function of time under vacuum and hydrogen atmospheres.

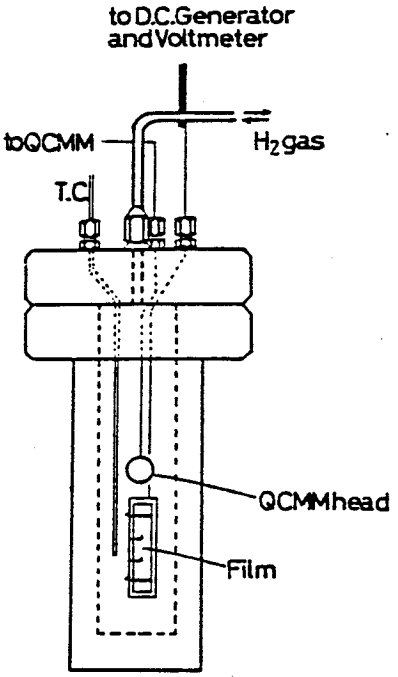

Fig. 1 The apparatus used for the electrical resistivity measurements and the QCMM frequency measurements.

4. 3. Results and Discussion

Electrical resistivities. Figures 2(a), (b) and (c) show the variation in electrical resistivity as a function of the time that hydrogen pressure was applied to $LaNi_5$ films of various thicknesses during the activation process.

The resistivity change in a thicker film (ca. 0.63 μm thick) is shown in Fig. 2(a). In the first cycle, the resistivity for the film kept rising when hydrogen gas was allowed into the system. After the evacuation of the system, the resistivity maintained a constant value. In the third cycle, the resistivity of the film increased immediately and then attained a constant value during the absorption process. During the desorption process, the resist-

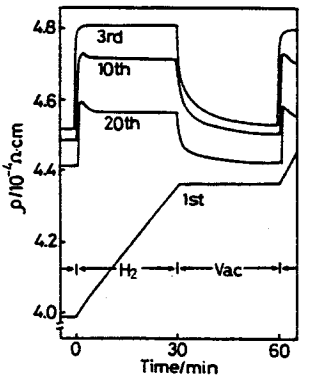

Fig. 2(a) Variation of resistivities as a function of time for the 0.63 μm thick $LaNi_5$ film.(at 313 K for 1st and 2nd cycle, at 363 K for other cycle, H_2 2.5×10^6 Pa)

ivity decreased rapidly at first and then gradually. During the tenth cycle the variation in the resistivity was almost the same as that during the third cycle. The corresponding increase and decrease was, however, quicker than that for the third cycle. After the first sudden increase, the resistivity decreased slightly.

Figure 2(b) illustrates the change in resistivity of a thinner film (ca. 0.20 μm thick). The behavior during the first cycle is similar to that of the third cycle for the thicker film. As the cycle was repeated, the rate of decrease in the resistivity (which occured after the increase when hydrogen was first admitted into the system) becomes faster. When the system was evacuated (as is seen from the results of the 10th cycle in the thicker film) there occured a sudden decrease in the resistivity. Then, the resistivity gradually increased.

Figure 2(c) displays the resistivity change in a thinnest film (ca. 3.8×10^{-2} μm thick). During the 10th cycle, there was no increase caused by introduction of hydrogen into the system. It was found that the resistivity change differs depending on the thickness of the film.

Figure 3(a) shows the variation of the resistivities for a relatively thick $SmCo_5$ film (thickness ca. 0.60 μm). When hydrogen was introduced into the system, there was a sudden increase in the resistivity, and the resistivitiy maintained a constant value. The behaviour of resistivity change was almost the same as that of the $LaNi_5$ film (Fig. 2(a)). However, as is shown in Fig. 3(b), the variation of resistivities for a thinner film was quite different from that for the $LaNi_5$ film(Fig. 2(b)).

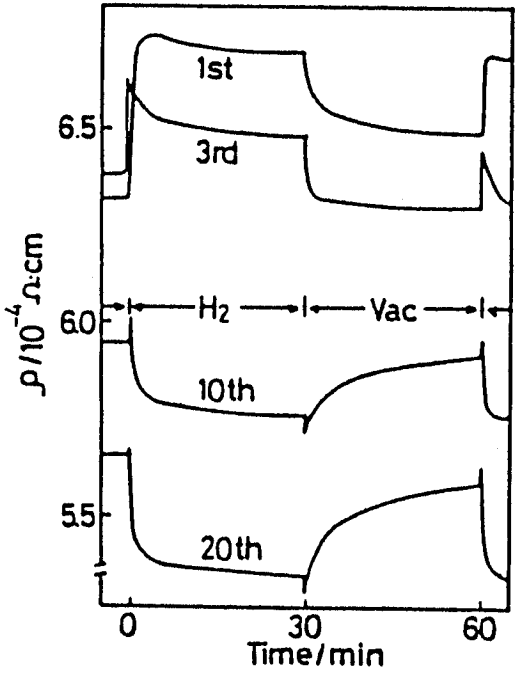

Fig. 2(b) Variation of resistivities as a function of time for the 0.20 μm thick $LaNi_5$ film.

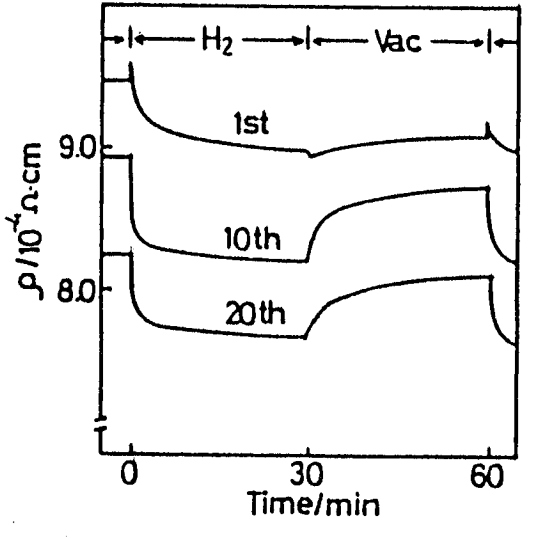

Fig. 2(c) Variation of resistivities as a function of time for the 3.8 $x10^{-2}$ μm thick $LaNi_5$ film.

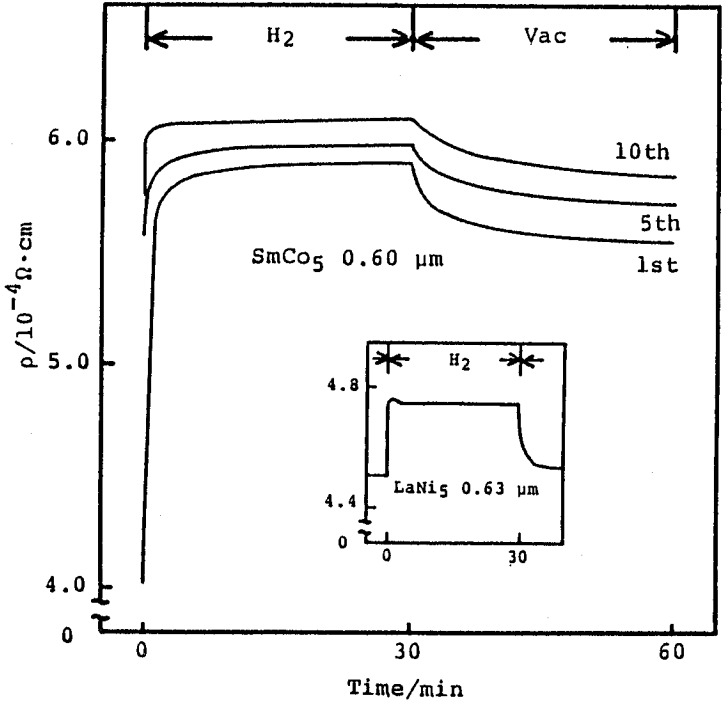

Fig. 3(a) Variation of resistivities for the 0.60 μm thick $SmCo_5$ film. (H_2 2.5×10^6 Pa, 363 K)

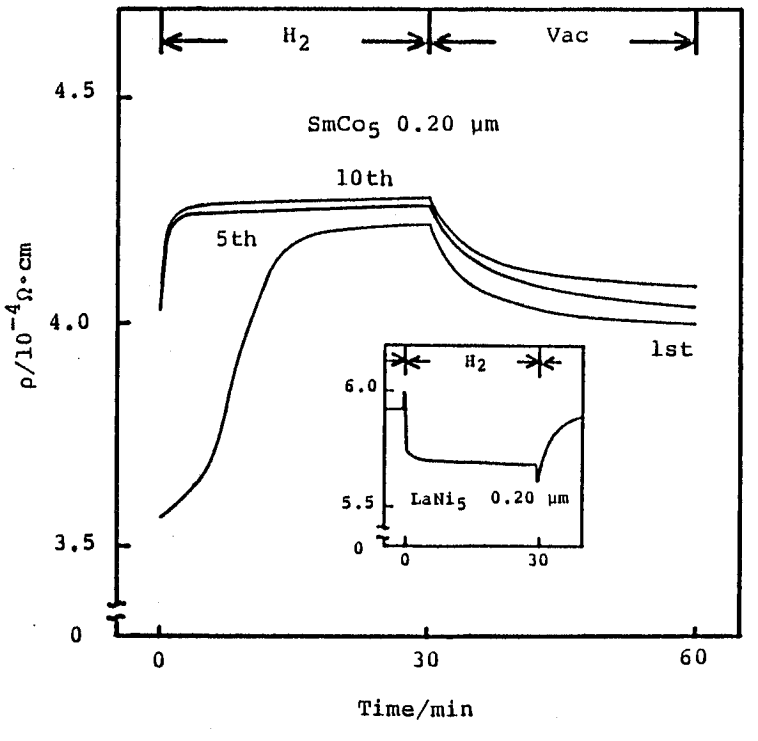

Fig. 3(b) Variation of resistivities for the 0.20 μm thick $SmCo_5$ film.

Figure 3(c) illustrates the variation of resistivities for a thinnest film(thickness ca. 2.0×10^{-2} μm). Introduction of hydrogen gas into the system the resistivity decreased steeply at first, and then gradually. The results were similar to those of the 0.2 μm thick $LaNi_5$ film.

The resistivity change in a thicker $LaCo_5$ film(0.50 μm thick) is shown in Fig. 4(a). In the first cycle, the resistivity for the film kept rising when hydrogen gas was allowed into the system. After the evacuation of the system, the resistivity decreased rapidly at first and then gradually. In the third cycle, the resistivity of the film increased immediately and then attained a constant value during the absorption process. During the desorption process, the resistivity first decreased suddenly and then gently. During the tenth cycle the variation in the resistivity exhibited almost the same behaviour that during the third cycle. The corresponding increase and decrease was, however, quicker than for the third cycle. These behaviour resembled that for the $LaNi_5$ film(0.63 μm thick, Fig. 2(a)).

As is shown in Figs. 4(b) and 4(c), a difference in the thickness of the films did not affect the shape of the resistivity change, though the rate of resistivity variation was changed.

Mechanism of hydrogen absorption-desorption. The explanation of the resistivity change is performed with two ways of thinking, i.e. the variation of concentration and mobility of conduction electrons(localization of electrons) and the changes in the density of states(delocalization of electrons). The

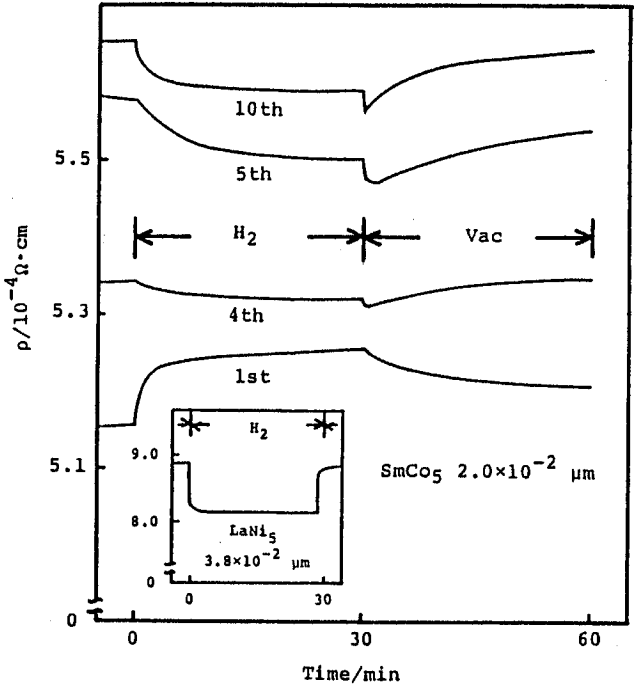

Fig. 3(c) Variation of resistivities for the 2.0×10^{-2} μm thick $SmCo_5$ film.

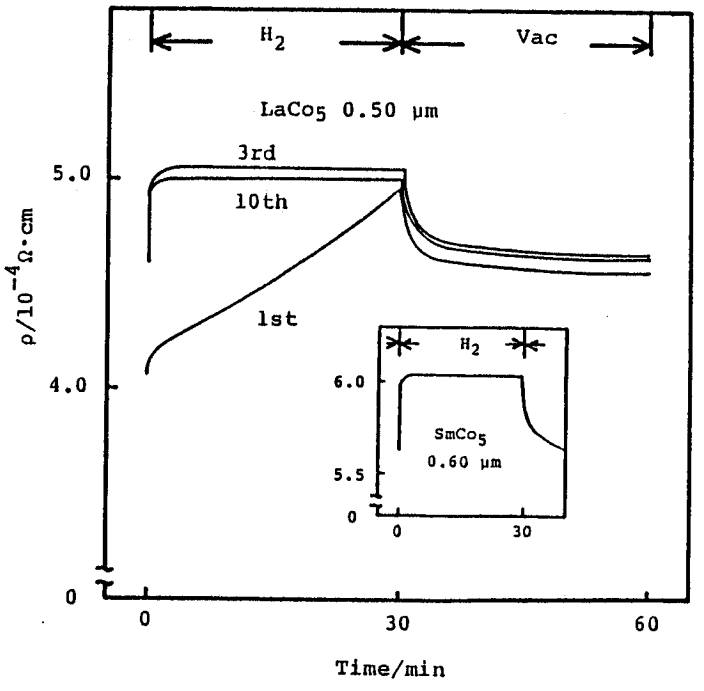

Fig. 4(a) Variation of resistivities for the 0.50 μm thick $LaCo_5$ film. (H_2 2.5×10^6 Pa, 363 K)

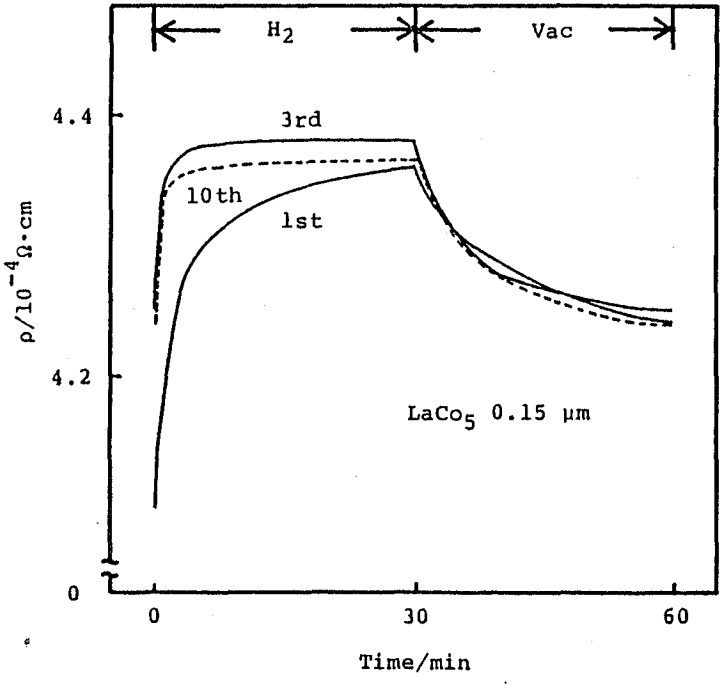

Fig. 4(b) Variation of resistivities for the 0.15 μm thick $LaCo_5$ film.

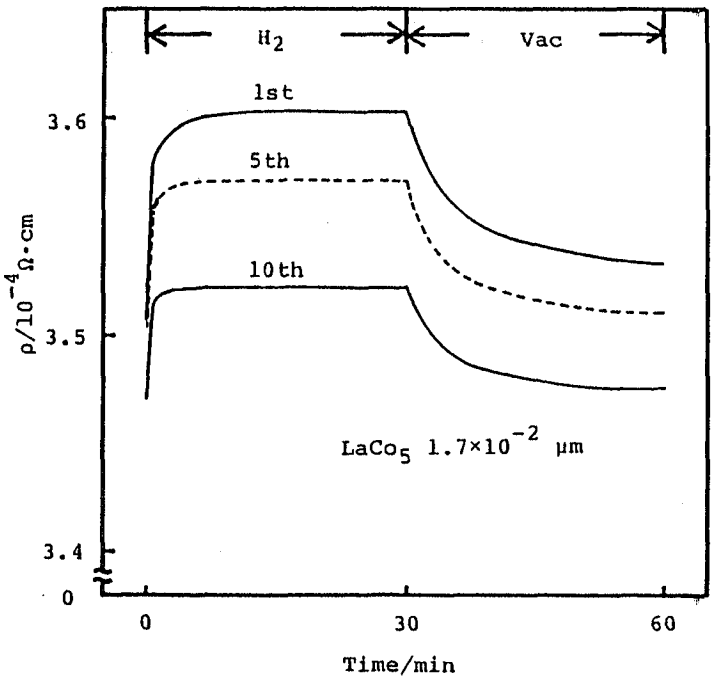

Fig. 4(c) Variation of resistivities for the 1.7×10^{-2} μm thick $LaCo_5$ film.

former was adopted to explain the mechanism of hydrogenation for the rare-earth alloys.

Hydrogen reacts with all of elements, and then forms hydrides or hydrogen compounds. The hydrides are clasified into three types, i.e. saline hydrides, metallic hydrides and covalent hydrides. Metallic hydrides have a metallic luster and the electrical resistivity which is similar to that of metals. This exhibits the properties of conduction electrons. Electrons captured from hydrogen atoms fill up the d-band of metal or become free electrons, while hydrogen atoms seem to become hydrogen anions. Rare-earth hydrides are the representative of the metallic hydrides. The formation mechanism of hydrogen anions-conduction electrons was used to clarify the mechanism of hydrogen absorption in the rare-earth alloys.

Figure 5(a) shows the representative shape of resistivity variation for the thicker $SmCo_5$ film. According to Wallace et al[5], the surface of $SmCo_5$ film is coated with Sm_2O_3 and precipitated cobalt. Hydrogen molecules are adsorbed on the surface and then dissociate into atoms. The dissociated hydrogen atoms reach the underlying $SmCo_5$ by diffusion in monatomic form along the Sm_2O_3-Co interface. Whereon the hydrogen atoms take on conduction electrons of $SmCo_5$. This reaction is represented by a formula $H + e^- = H^-$. Decrease in the number of electrons in the conduction band of the $SmCo_5$ causes a resistivity increase. The dissolved hydrogen anions diffuse in the film and then react with Sm in $SmCo_5$, giving a high conductivity hydride. The presence of the high conduc-

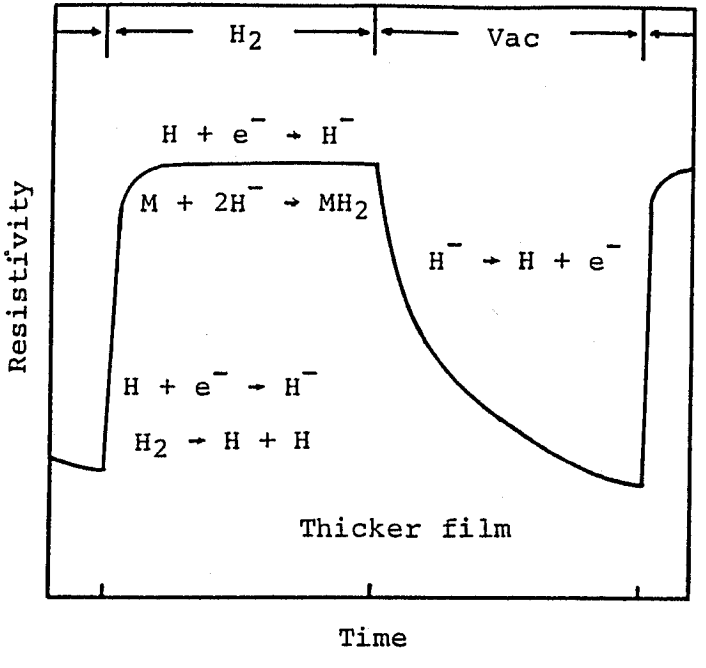

Fig. 5(a) Mechanism of hydrogen absorption-desorption for thicker $SmCo_5$ films.

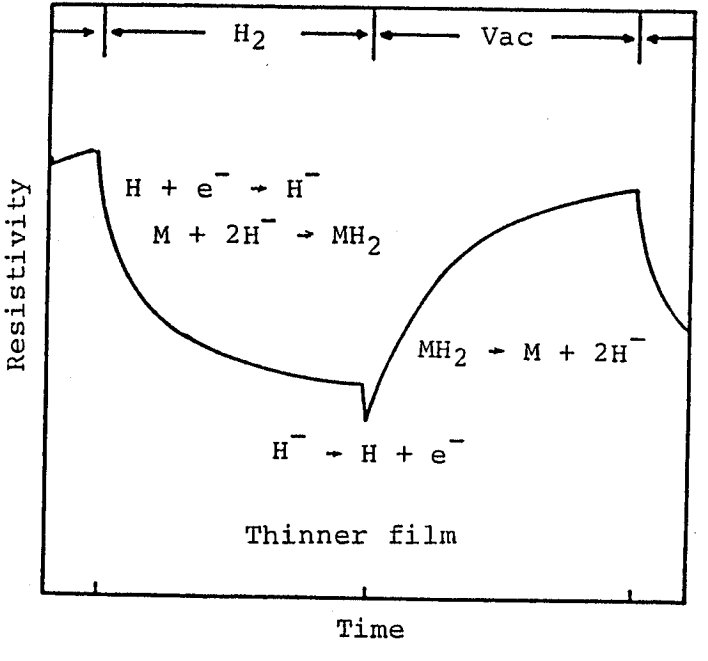

Fig. 5(b) Mechanism of hydrogen absorption-desorption for thinner $SmCo_5$ films.

tivity hydride lowers the resistivity of the film. Since the formation of hydrogen anion is balanced by the formation of high conductivity hydride, the resistivity is maintained a constant value. When the system is evacuated, the resistivity decreases at first rapidly and then slowly, because some dissolved hydrogen anions are released as hydrogen molecules leaving their electrons in the conduction band of the metal. Figure 5(b) illustrates the variation of the resistivity for the thinner film(thickness ca. 2.0×10^{-2} μm). Introduction of hydrogen gas into the system decreases the resistivity at first steeply and then gradually, suggesting that dissolved hydrogen anions react with Sm in $SmCo_5$ and form the high conductivity hydride. When the system is evacuated, there occurs a sudden decrease in resistivity because of the removal of the residual hydrogen anion. After the decrease, the resistivity increases gradually due to decomposition of the hydride.

For $SmCo_5$ and $LaNi_5$ films, a difference in the thickness of the films is found to affect the shape of the resistivity change. The amount of the resulting high con-

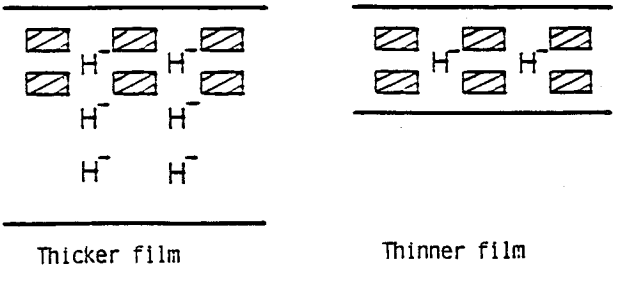

Fig. 6 Relationship between the high conductivity hydride and the hydrogen dissolved slightly conductive metal.

ductivity hydride phase seems to be constant(Fig. 6) with varying film thickness. For the thicker film, the amount of the H^- dissolved phase, which is less conductive, is quite large and the effect of this phase on the resistivity of the film is predominant with respect to that of the coexisting high conductivity hydride. Therefore, the resistivity increases. For the thinner film, the effect of the high conductivity hydride is predominant and the resistivity decreases. For the $LaCo_5$ films, however, a difference in the thickness of the films does not affect the shape of the resistivity variation. This is because the $LaCo_5$ films form less hydride than the $LaNi_5$ films. The high conductivity hydride seems to be LaH_2. Since the $LaCo_5$ films absorb less hydrogen than the $LaNi_5$ films, the amount of LaH_2 formed in the $LaCo_5$ films is less than that in the $LaNi_5$ films.

We have assumed a mechanism in which the formation of a hydride(LaH_2), which is a good conductor, play a crucial role in the understanding of the resistivity changes. The behaviour of the resistivity change for $LaNi_5$ and $LaCo_5$ was much different from that for $SmCo_5$. The resistivity in vacuo for $LaNi_5$ and $LaCo_5$ films decreased with repeated hydrogen absorption-desorption cycle. This seems to be attributable to the formation of the good conductor LaH_2. In contrast, for $SmCo_5$ films, as is shown in Fig. 3, the resistivity in vacuo increased. Samarium unlike lanthanum exhibits two valencies, i.e. Sm^{2+} and Sm^{3+}. When Sm^{3+} forms SmH_2, the hydride seems to be a high conductivity hydride.

However, in the case of Sm^{2+}, the resulting hydride is an insulator. The insulator also seems to accumulate with repeated hydrogen absorption-desorption cycle, so that the base line of resistivity in vacuo increases. Therefore, it was assumed that the trivalent rare-earth elements, such as La^{3+} and Sm^{3+} form high conductivity hydrides and the hydrides have an influence on the resistivity of the films.

The second explanation for the resistivity change on hydrogenation is that the band structure itself might be changed[22].

As is shown in Table 1, in the case of a thickness of 0.2 μm, the resistivity of only the $LaNi_5$ film decreased during hydrogen absorption process. Therefore, it is found that the $LaNi_5$ film is easy to form the high conductivity hydride compared with the other films. For the thinnest films, the resistivity of only the $LaCo_5$ film increased during hydrogen absorption process, suggesting that the $LaCo_5$ film is difficult to form the high conductivity hydride in comparison with other two films.

Table 1

Film thickness \ Films	$LaNi_5$	$SmCo_5$	$LaCo_5$
0.2 μm	−	+	+
2×10^{-2} μm	−	−	+

− The resistivity decreases during hydrogen absorption procrss.

\+ The resistivity increases during hydrogen absorption process.

$$LaNi_5 > SmCo_5 > LaCo_5$$

Activation energy for hydrogen absorption.

The time dependence of resistivity in the initial stage of absorption at various temperatures is shown in Fig. 7. The rate of absorption was in the following order; $LaNi_5$ > $SmCo_5$ > $LaCo_5$. The reaction rate constants were obtained from the slopes of the straight lines in Fig. 7[23]. Figure 8 illustrates Arrhenius plots of the rate constants for hydrogen absorption of various films having different thicknesses. The value of activation energy was about 60 $kJmol^{-1}$ for all films independent of the kind of alloy and the film thickness. These alloy films, therefore, give the same mechanism of hydrogen absorption.

4. 4. Summary

Electrical resistivity measurements for the deposited films were performed under hydrogen atmospheres. Resistivities initially increased and then maintained a constant value or decreased during the hydrogen absorption process. As for the desorption process, the reverse phenomena were observed.

The formation mechanism of hydrogen anions-conduction electrons was used to explain the mechanism of hydrogenation for the rare-earth alloys. The resistivity changes suggest that the following steps take place during hydrogen absorption. The dissociated hydrogen atoms take on the conduction electrons of the metals and become the hydrogen anions. The number of electrons in the conduction band of the metals decreases, and consequently the resistivity increases, followed by the occurrence of the formation of a high conductivity hydride.

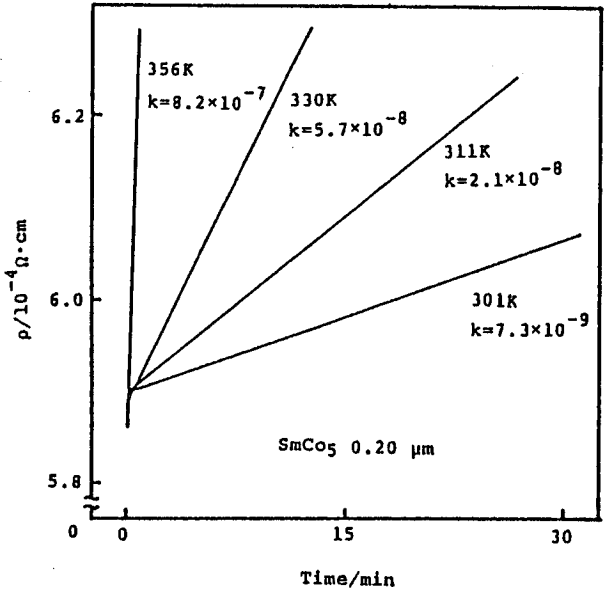

Fig. 7 The time variation in the electrical resistivity at various temperatures. (H_2 2.5x10^6 Pa)

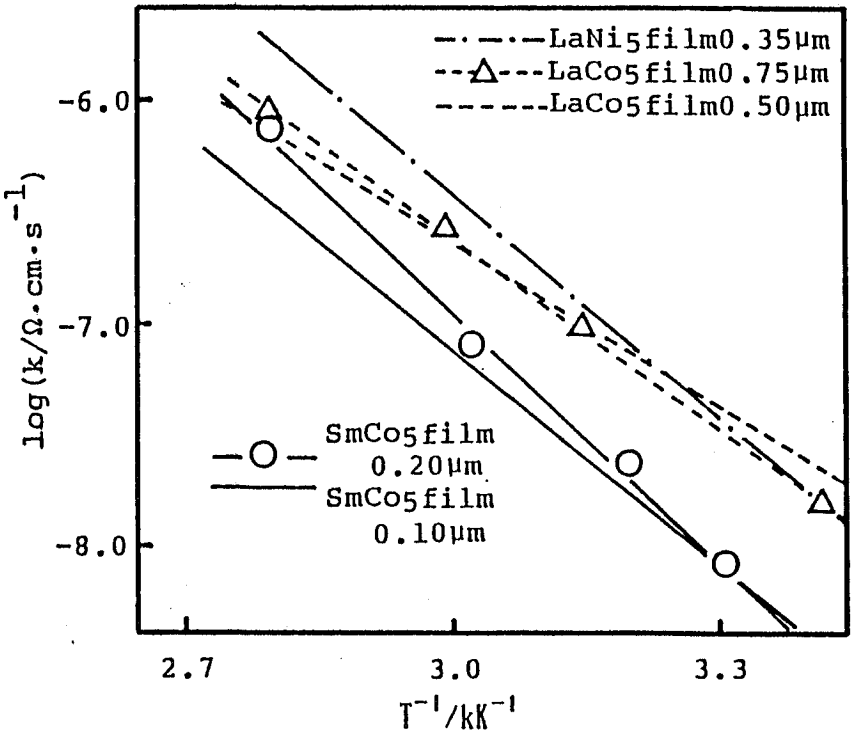

Fig. 8 Arrhenius plot for hydrogen absorption in several times.

Chapter 5

DETERMINATION OF HYDROGEN CONTENT IN RARE-EARTH ALLOY FILMS USING A QUARTZ-CRYSTAL MASS-MONITORING(QCMM) METHOD

5. 1. Introduction

It is necessary to know the hydrogen content of the film. However, conventional measuring techniques, such as a volumetric method, are not applicable to thin films because these techniques require large sample volumes.

The most-sensitive instrument for measuring the hydrogen content in thin films is the QCMM. Bucur and Flanagan[24], Frazier and Glosser[25] have initially demonstrated its application in measuring the hydrogen/metal atom ratio with changes in hydrogen pressure and system temperature for deposited palladium films. We have also used this technique to determine the quantity of hydrogen uptake for $LaNi_5$ and $LaCo_5$ films of various thicknesses. Furthermore, the relationship between hydrogen concentration and film thickness or hydrogen pressure was investigated.

5. 2. Experimental

Preparation of films. Substrates were quartz crystal discs which were the standard film thickness monitors, with diameters of 17.3 mm and a thickness of about 0.3 mm, and had an AT-cut with a frequency constant of 1.67 MHz mm^{-1} and a vibrational frequency of 6 MHz.

$LaNi_5$ films were prepared by means of flash-evaporation-deposition and sputtering methods. The evaporation method was used to prepare $LaCo_5$ films.

Measurements of properties. After sample preparation and transfer of the samples into the high-vacuum apparatus, the sample was exposed to hydrogen in pressure increments varying from vacuum to 2.5×10^6 Pa at 333 K or 363 K, the frequency shift was measured with QCMM(NICHIDEN ANELVA EVM 32B) with an error of less than 3 % to the frequency change of 300 kHz. The minimum sensitivity for this apparatus is 20 Hz. The amounts of hydrogen absorption taken up by the $LaNi_5$ films were determined by the relationship between the frequency change during film deposition and the deposited mass. Since the frequency changed only with pressure, the frequency shift was calibrated by the shift which was measured with helium under the same condition because helium was not absorbed by $LaNi_5$. For 1.8 μm deposited $LaNi_5$ film, when hydrogen was introduced into the system, the frequency shifted about 350 Hz to the low frequency side, while the frequency changed about 100 Hz to the higher side when the measurement was performed using helium. Therefore, the actual shift(450 Hz)

due to the hydrogen absorption was obtained by addition of the frequency shift(100 Hz) depending on the pressure to the shift(350 Hz) when hydrogen was supplied.

5. 3. Results and Discussion

5. 3. 1. Hydrogen content in deposited $LaNi_5$ films

Figure 1 shows the hydrogen content in an $LaNi_5$ film (2.0 μm thick) for repeated hydrogen absorption-desorption cycle at 333 K. The amounts of hydrogen absorption taken up by the $LaNi_5$ film at each cycle were constant at about 2.3 ± 0.4 $H/LaNi_5$.

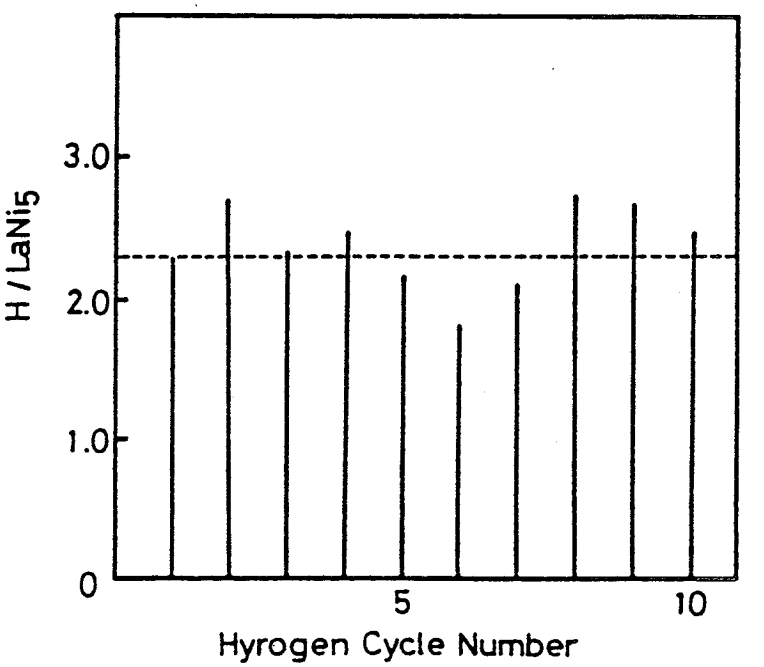

Fig. 1 Hydrogen content in the deposited $LaNi_5$ film(thickness 2.0 μm).
(H_2 2.5×10^6 Pa, 333 K)

For more thinner film(1.1 μm thick), as is shown in Fig. 2, 1.1 ± 0.1 hydrogen atoms for a formula weight of $LaNi_5$ were absorbed by the film at each cycle. Thus, it was found that the hydrogen content was much different between these two films with different thicknesses.

The same measurement was performed for the films having various thicknesses. The amounts of hydrogen were 0.7 ± 0.2, 1.4 ± 0.2 and 2.0 ± 0.1 for films of 0.6, 1.5 and 1.8 μm thickness, respectively. Figure 3 indicated the relationship between the hydrogen concentration increased with increasing film thickness.

The $H/LaNi_5$ ratios for the films were very small in comparison with that for a crystalline sample, i.e. 7 $H/LaNi_5$ [3]. It seems that there is an effect from the oxide layer which can not absorb hydrogen. However, the effect appears to be minor because the thickness of the oxide layer is very small, i.e. 10^{-2} μm compared with the total film thickness. The amorphous state of the film structure seems to be one of the reasons why the hydrogen content in the film is small, because for the amorphous film, the number of site which can be occupied with hydrogen atoms decreases. The results for the Pd-Si, Fe-Ti and Zr-Ni amorphous alloys are analogous to ours[26-29]. A lattice of $LaNi_5$ expands when it absorbs hydrogen. The film is, however, strongly fixed on the substrate and can not expand easily and does not absorb much hydrogen. It was reported that for the Pd thin film, the cubical expansion decreases due to the fixation of the film by the substrate[30].

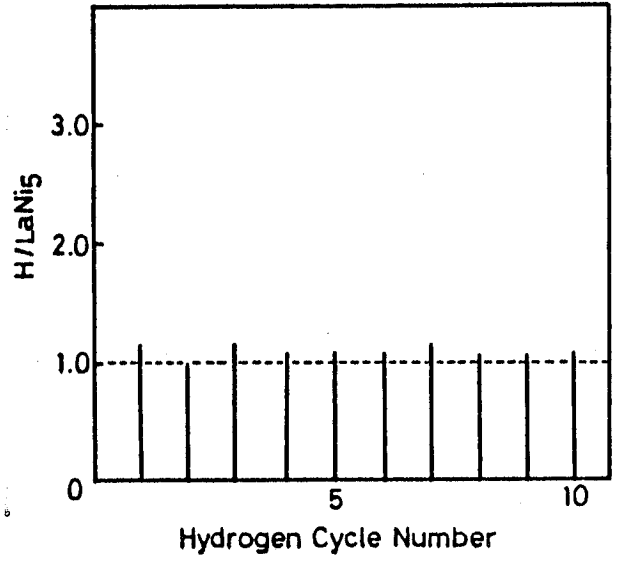

Fig. 2 Hydrogen content in the deposited $LaNi_5$ film(thickness 1.1 μm).

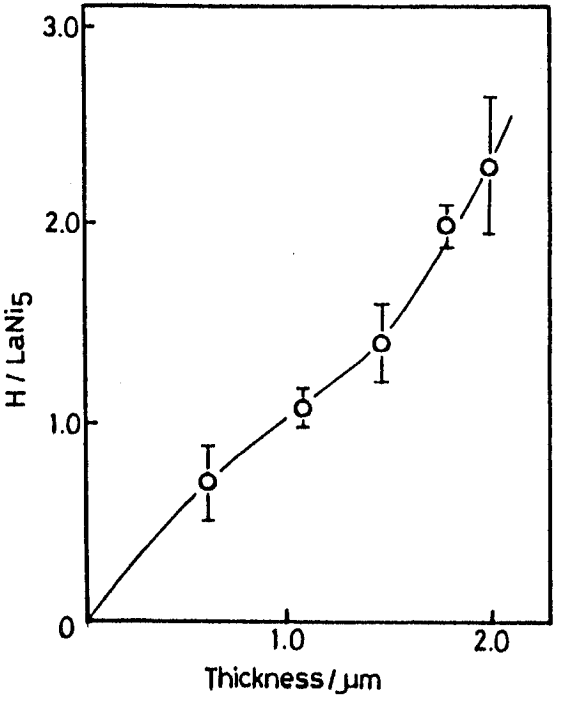

Fig. 3 Hydrogen content in the $LaNi_5$ film vs. film thickness.

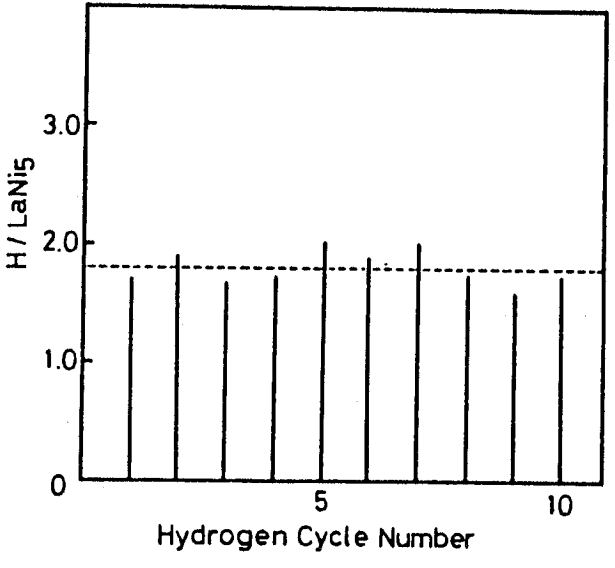

Fig. 4 Hydrogen content in the deposited $LaNi_5$ film(thickness 2.0 μm) at 363 K.

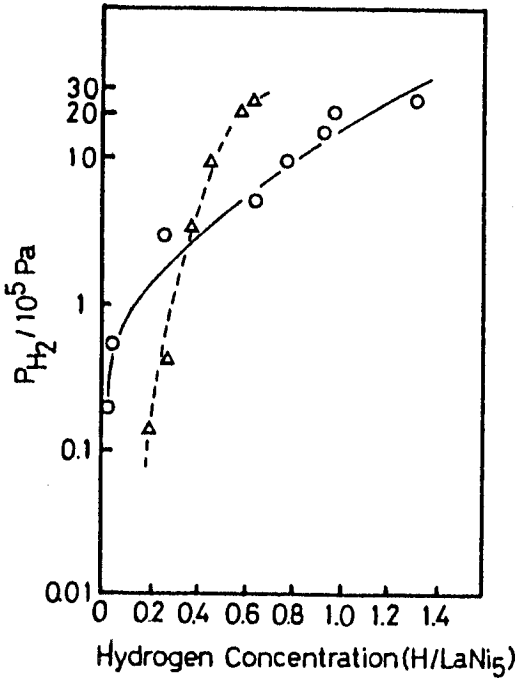

Fig. 5 Pressure-concentration isotherms for $LaNi_5$ films at 333 K.
(○) 1.5 μm, (△) 0.6 μm.

For the 2.0 μm thick $LaNi_5$ film(Fig. 4), the hydrogen content was also measured at 363 K and its value was about 1.8 ± 0.2 $H/LaNi_5$. Thus, the hydrogen content at a higher temperature was smaller than that at a lower temperature.

As is shown in Fig. 5, the hydrogen concentration(H/M) in $LaNi_5$ films increases with increase in hydrogen pressure on 0.6 and 1.5 μm films. No pressure plateau appears on the PC-curves, though it is usually observed in a crystalline sample($8x10^5$ Pa, at 333 K). The results for Zr-Ni and Fe-Ti amorphous alloys[26-28] are analogous to our results. It can be assumed that the absence of a pressure plateau is one of the features of an amorphous alloy.

5. 3. 2. Hydrogen content in sputtered $LaNi_5$ films

The hydrogen content in the 3.1 μm thick film was 2.4(0.1) for a formula weight of $LaNi_5$ on an average to 10 cycles of hydrogen absorption-desorption process at 363 K and an atmosphere of $2.5x10^6$ Pa hydrogen. For the 1.3 μm and the 0.93 μm thick films, the amounts of hydrogen taken up by these films were 2.4(0.3) $H/LaNi_5$ and 1.5(0.1) $H/LaNi_5$, respectively. The values in parentheses indicates the standard deviation.

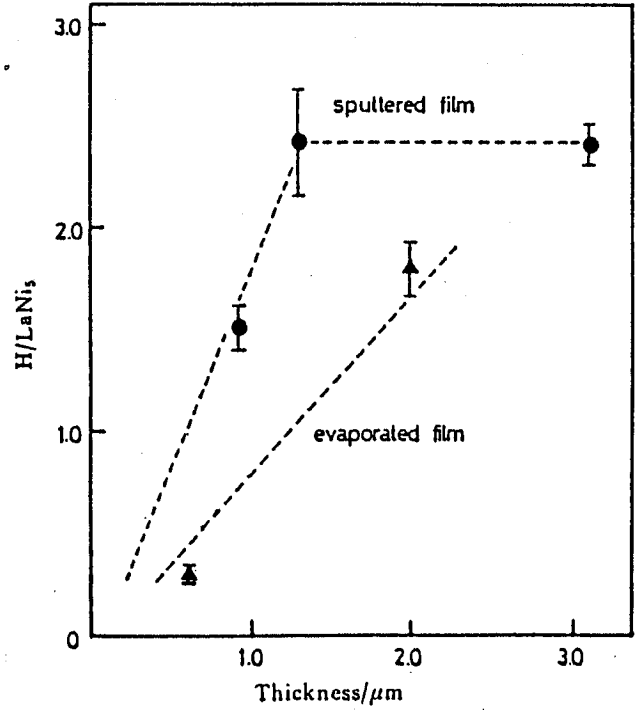

Fig. 6 Hydrogen concentration vs. thickness of $LaNi_5$ films.
(H_2 2.5×10^6 Pa, 363 K)

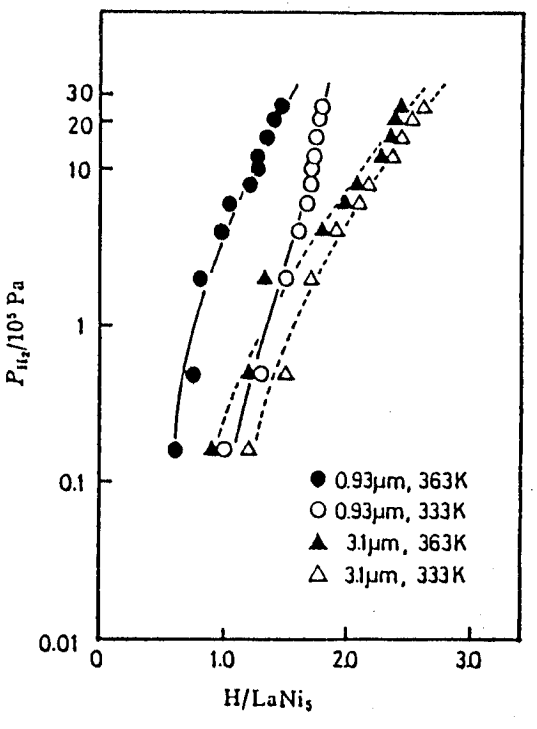

Fig. 7 Pressure-concentration isotherms for $LaNi_5$ sputtered films.

The relationship between the hydrogen content and the film thickness is illustrated in Fig. 6. For the above 2 μm thick sputtered film, the measurement of the hydrogen content could not perform because an oscillation of a quartz-crystal element had been stopped. The sputtered films can absorb more hydrogen than the deposited films for the below 2 μm thick films having a same thickness. This appears to be that since the sputtered film takes on a crystalline character, the number of hydrogen sites on the sputtered films is larger than that on the deposited film. Recently, Uchida et al reported that the film was annealed at 673 K, so that the hydrogen concentration in the film increased in comparison with that in the film before annealing[31].

The hydrogen concentration increased with enlarging the film thickness due to increase in the crystallinity of the film. For the sputtered film the hydrogen concentration maintained a constant value at nearly 1.3 μm because the progress of the crystallization appeared to be stopped. The deposited film is difficult to crystallize, so that the crystallinity was varying even at above 2 μm. The progress of the crystallization may be stopped at about 3 μm and the hydrogen concentration is assumed to maintain a constant value which is lower than that of the sputtered film.

The pressure dependence of the hydrogen concentration ($H/LaNi_5$) in the sputtered films at 333 K and 363 K is shown in Fig. 7. The hydrogen concentration was found to increase monotonously with increasing the hydrogen pressure despite the variation in temperatures and film thicknesses.

Therefore, the single phase which dissolves hydrogen anions seems to be predominant. The results for the deposited films are analogous to ours.

As far as the temperature dependence of the isotherm is concerned, the hydrogen content at a higher temperature was less than that at a lower temperature under the same hydrogen pressure.

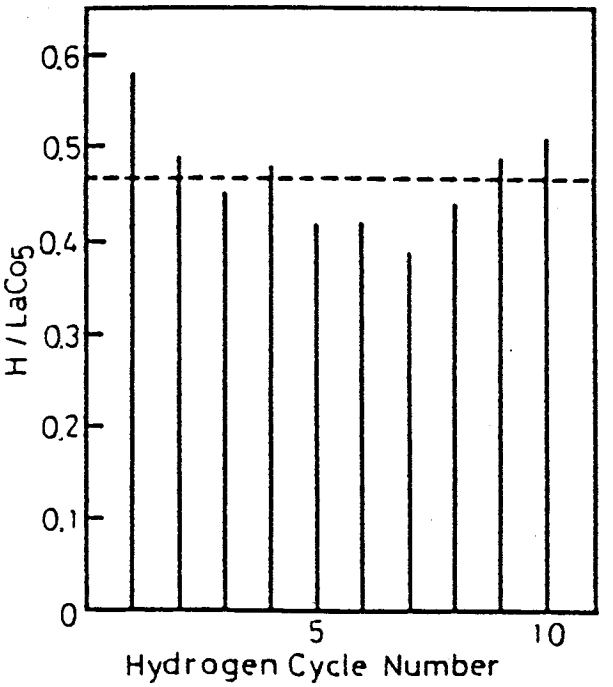

Fig. 8 Hydrogen content in the deposited $LaCo_5$ film(thickness 2.1 μm) at 333 K.

5. 3. 3. Hydrogen content in deposited $LaCo_5$ films

Figure 8 shows the hydrogen content in the $LaCo_5$ film (2.1 μm thick) for repeated hydrogen absorption-desorption cycles at 333 K. The amounts of hydrogen taken up by the

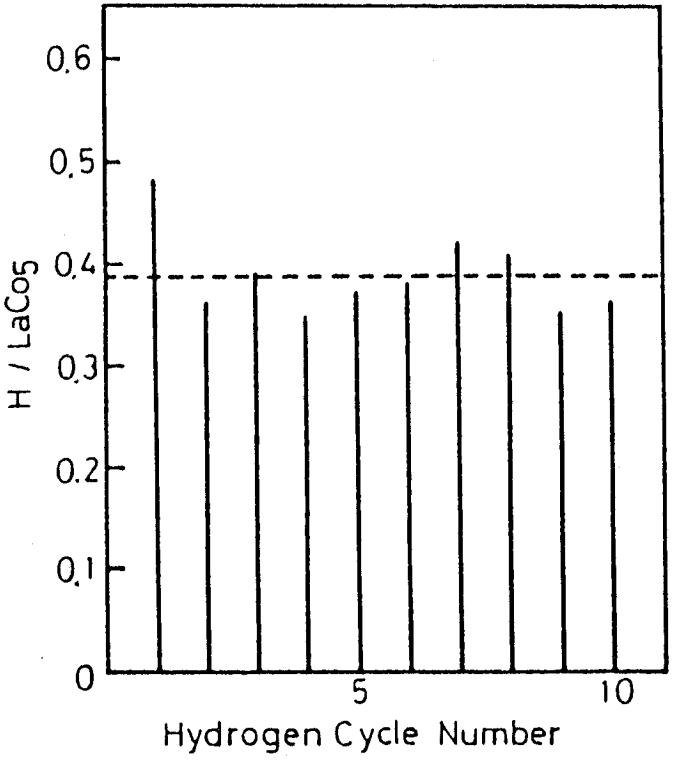

Fig. 9 Hydrogen content in the deposited $LaCo_5$ film(thickness 1.4 μm) at 333 K.

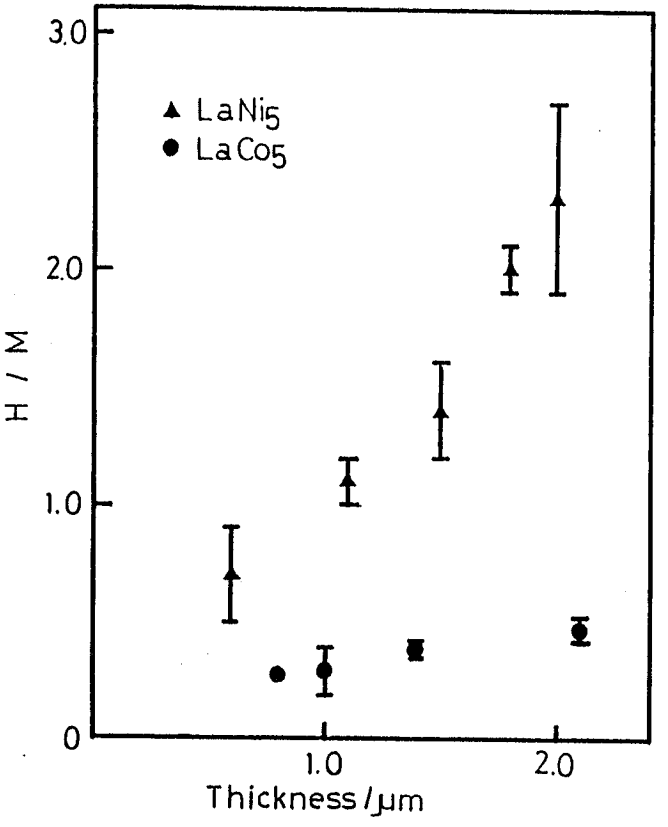

Fig. 10 Hydrogen concentration at 333 K vs. thickness of $LaNi_5$ and $LaCo_5$ films.

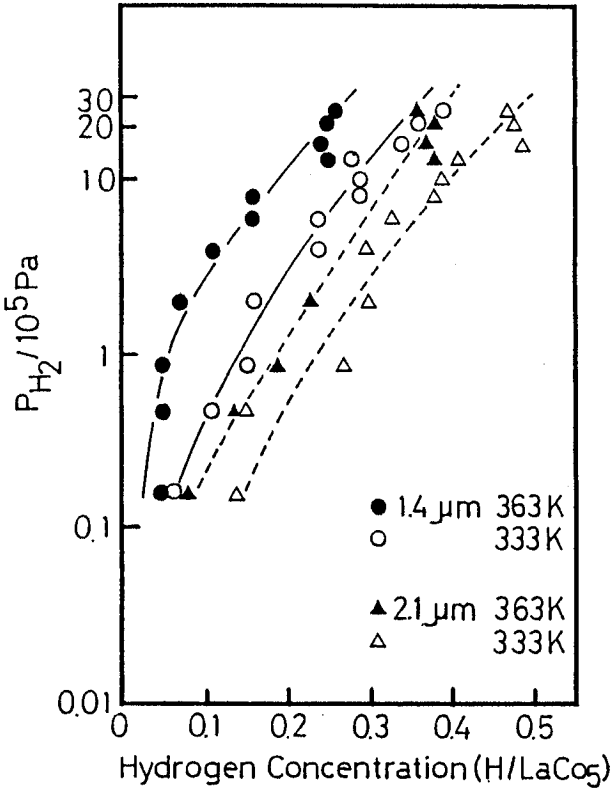

Fig. 11 Pressure-concentration isotherms for $LaCo_5$ films.

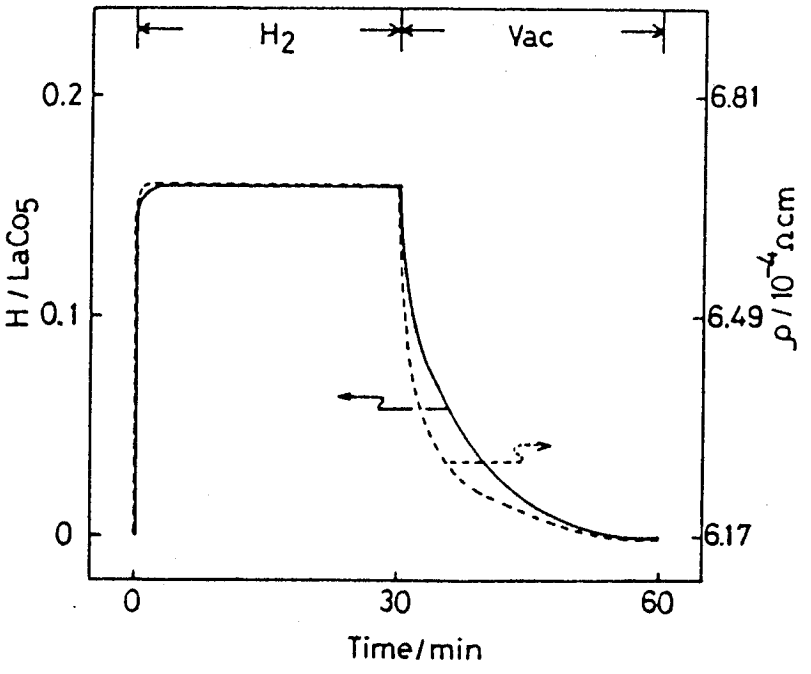

Fig. 12 Comparison of the variation in resistivity with time and the variation in hydrogen content of the film with time at 363 K.

film at each cycle remained constant at about 0.47 ± 0.05 $H/LaCo_5$. A large amount of hydrogen was absorbed in the film for the initial cycle only. This phenomenon coincides with the result of the electrical resistivity measurements (Fig. 4 in Chapter 4). A similar experiment was performed for the thinner film(1.4 μm thick), giving 0.39 ± 0.04 hydrogen atoms for one formula weight of $LaCo_5$(Fig. 9).

The relationship between the hydrogen content and the film thickness is illustrated in Fig. 10. The $H/LaCo_5$ ratios for the $LaCo_5$ films less than 2.1 μm thickness were very small in comparison with that for a crystalline sample, i.e. 4.2 $H/LaCo_5$[2].

For crystalline samples, $LaNi_5$ absorbs more hydrogen than $LaCo_5$[2]. This tendency was also observed in film samples.

The pressure dependence of the hydrogen concentration ($H/LaCo_5$) in the $LaCo_5$ films at 333 K and 363 K is shown in Fig. 11. The hydrogen concentration was found to increase monotonously with increasing hydrogen pressure despite the variation in temperature and film thickness.

In Fig. 12 the variation in resistivity of the film 0.8 μm thickness is compared with that in hydrogen content of the film. A relatively good agreement is found.

5. 4. Summary

The hydrogen content in the films obtained was found to be smaller than that in crystalline samples. The hydrogen

concentration in the $LaNi_5$ films was much larger than that in the $LaCo_5$ films. In pressure-composition isotherms, the hydrogen concentration increased monotonously with pressure despite the variations both in temperature and in film thickness suggesting that the single phase which dissolves hydrogen anions seems to be predominant.

Chapter 6

STUDIES ON HYDROGEN PERMEABILITY FOR VARIOUS METALS USING THE COLORING OF AMORPHOUS WO_3 WITH HYDROGEN PENETRATED THROUGH SANDWICH-TYPE FILMS(a-WO_3/METAL /$LaNi_5$)

6. 1. Introduction

A thin film of amorphous tungsten oxide a-WO_3 has been studied because of its electrochromism[32-34]. Coloration of the transparent film has been known to occur as a result of a double injection of protons and electrons, and the formation of tungsten bronzes.

When hydrogen was applied to an $LaNi_5$ film vapor deposited on a-WO_3, it was observed that the a-WO_3 film changes its body color[35]. This is because the dessolved hydrogen permeated through the $LaNi_5$ film and the hydrogen penetrated into the a-WO_3, reducing W^{6+} in the a-WO_3 to W^{5+}. Another sample prepared by depositing a copper thin film on the a-WO_3 and then an $LaNi_5$ thin film on top of the copper layer(a-WO_3/Cu/$LaNi_5$). The a-WO_3 adopted the blue color only under the area covered by the $LaNi_5$ layer when hydrogen was introduced into the system. The phenomenon seems to be suitable as an indication of hydrogen permea-

bility in metals.

In this paper the results are reported of studies on the hydrogen permeability in various metals selected from each group of the periodic table.

6. 2. Experimental

Tungsten oxide films were deposited on glass substrates by evaporation of WO_3 powder(WAKO PURE CHEMICAL INDUSTRIES, LTD.) in a tungsten boat at 2.3×10^3 K. The thermal evaporation was carried out under a vacuum below 1.3×10^{-2} Pa. The temperatures of the films during evaporation were in the range of 300-420 K, measured by a chromel-alumel thermocouple. The distance between the substrate and the tungsten boat was 0.2 m.

Mg, Ti, Cr, Mn, Fe, Co, Cu, Ag. Au, Zn and Al films of 0.2 μm thickness were prepared on a-WO_3 coated glass substrates by a vacuum evaporation and then forming an $LaNi_5$ film was formed using the flash-evaporating method. Thus, multilayered samples were obtained which consisted of the a-WO_3 film, the metal film and the $LaNi_5$ film. Figure 1 shows a structure of the sample.

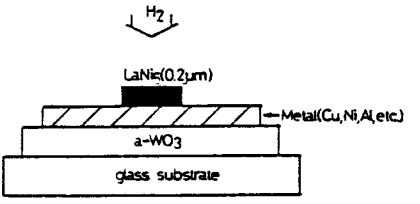

Fig. 1 Schematic representation of test piece.

Ni, Pd and Pt films of 0.2 μm thickness were prepared on a-WO_3 coated glass substrates by a vacuum evaporation or a sputtering. These films were not covered with the $LaNi_5$ film. Hydrogen permeability of the metals was directly compared with that of $LaNi_5$.

The hydrogen pressure of 2.0×10^6 Pa was applied to the samples in a stainless steel vessel at about 350 K. The progress of coloration of the a-WO_3 film was observed at a given interval of elapsed time.

6. 3. Results and Discussion

Figure 2 represents the structure of the multilayered films which consist of copper and $LaNi_5$ films. The films are denoted A, B, C, D and E. After hydrogen was applied to the sample for 15 min, it was confirmed that rates at which coloration had proceeded were in the following order E > B > D > C > A. E showed the deepest shade of blue of all the films, while the color of the a-WO_3 on A was hardly changed. Interestingly, B displayed the next deepest shade of blue to E.

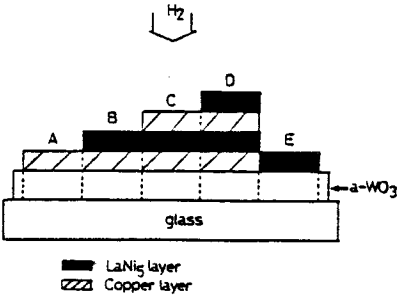

Fig. 2 Composition of the multilayered films.

$LaNi_5$ can absorb hydrogen in extremely large quantities, leading to concentration higher than those in liquid hydrogen at 4 K. Even copper whose hydrogen permeability is very small seems to be permeable because the hydrogen concentration on the surface of copper becomes very high. Furthermore, hydrogen from $LaNi_5$ may be in the atomic state and no activation energy is needed for dissociation of the hydrogen molecules on the surface of the copper. These explanations are supported by the fact that the hydrogen permeability of the films whose surfaces were coated with copper such as A and C was small.

A sample plate, as illustrated in Fig. 3, was used to investigate the effects of copper thickness on the hydrogen permeability. Figure 3 also shows the coloration progress of the a-WO_3 after a lapse of time. The relationship between the time required for a given degree of coloration and the thickness of the copper layer is shown in Fig. 4. Coloration was observed for copper films as thick as 2.0 μm. The time required for coloration to appear increased with increasing thickness of the copper layer. The diffusion of hydrogen in the copper layer seems to be the rate-determining step because the square root of the time required for coloration is approximately proportional to the thickness of the copper layer. The coloring of the a-WO_3 firstly took place only under the area covered with the $LaNi_5$ layer. For the 0.2 μm thick copper film, the blue color of the area covered by $LaNi_5$ had to become sufficiently deep before the surroundings became colored. When

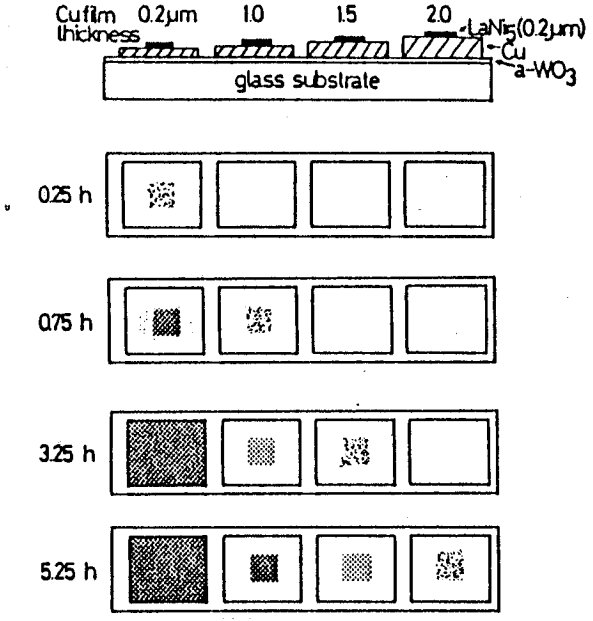

Fig. 3 Effects of the thickness of the copper film on the hydrogen permeability.

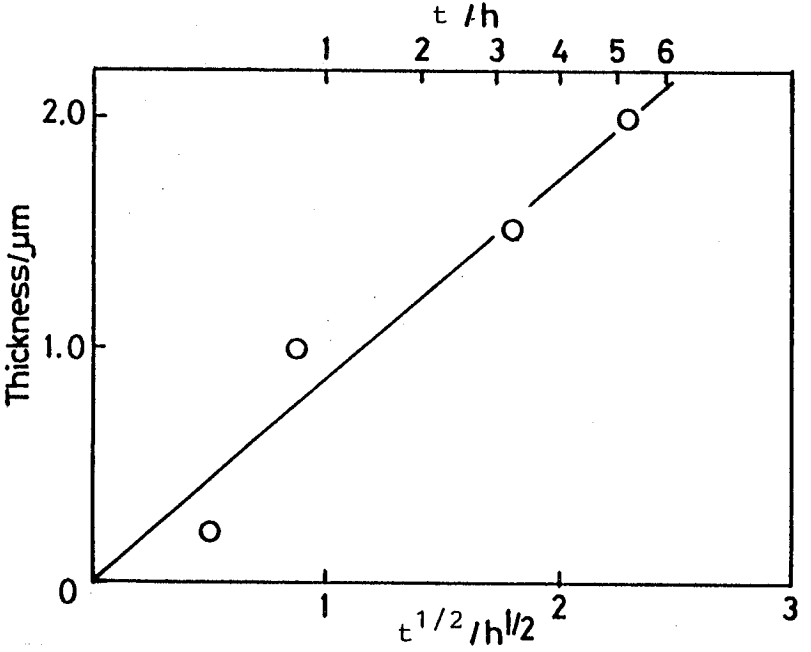

Fig. 4 Relationship between the thickness of the copper layer and the time required for the coloration of the a-WO_3 layer.

the hydrogen concentration between the copper layer and the a-WO_3 layer became adequately high, the concentration gradient needed for the diffusion of hydrogen could be generated at the inerface between the a-WO_3 layer and the copper layer. Consequently, the coloring of the surroundings seems to be taking place as a result of the diffusion of hydrogen at the interface. The hydrogen mobility at the interface seems to be very great. The coloring of the a-WO_3 did not occur at the uncovered area because the mobility at the area is very small. The films, except for 0.2 μm thick one, became blue only under the area coated with $LaNi_5$ layer. It may be considered that since the hydrogen concentration between the copper layer and the a-WO_3 layer was low, a sufficiently high concentration gradient in the a-WO_3 layer was not generated.

As mentioned above, it was found that if the metals which absorb hydrogen with difficulty, such as copper, are covered with $LaNi_5$, the hydrogen in the $LaNi_5$ is easily dissolved into the copper. Therefore, the coloration progress of the sandwich-type film(a-WO_3/Metal/$LaNi_5$) seems to indicate the hydrogen permeability of various metals.

We selected a few metals from each group of the periodic table in order to estimate their hydrogen permeability. The permeability decreased in the following order:

$$\begin{bmatrix} LaNi_5 \\ Pt \\ Pd \end{bmatrix} > Fe > \begin{bmatrix} Ni \\ Co \\ Ti \end{bmatrix} > Mn > Cu > \begin{bmatrix} Mg \\ \\ Cr \end{bmatrix} > Al > \begin{bmatrix} Au \\ Ag \\ Zn \end{bmatrix}$$

(1) (2) (3) (4) (5) (6) (7) (8)

Hydrogen solubilities measured under a pressure of 10^5 Pa at about 900 K vary as follows[36]:

$LaNi_5$ > Ti > Pd >> Mg > Mn > Ni > Fe > Co > Cu > Cr > Al > Pt > Ag > Zn > Au

Metals which absorb hydrogen in large quantities do not necessarily exhibit a high rate of hydrogen diffusion. The rate of hydrogen diffusion in the metals decreases in the following order: Pd > Fe, Al > Ni, $LaNi_5$ > Cu > Ti [36,37].

The order of hydrogen permeability obtained was discussed from viewpoint of the hydrogen solubility and the hydrogen diffusibility. The group of gold, silver and zinc(8) showed the least hydrogen permeability. This is because the hydrogen solubility of these metals is extremely low. As hydrogen could not reach the a-WO_3 layer, the coloration did not take place. Aluminum(7) gave a poor permeability next to (8) group. Although the hydrogen solubility of aluminum is low, the rate of diffusion of Al is large and comparable with that in iron. It is important to take account of the formation of oxide on the surface of metal film, because the metal films were exposed to air during the preparation of sample. Metals which exhibit passivity seem to form a dense oxide layer. The oxide layer is considered to be an obstacle to the absorption of hydrogen. Aluminum is known to form the passive layer[38]. Therefore, the hydrogen permeability was low in spite of possessing the large diffusivity. The hydrogen permeability of chromium(6) was in between those of copper and aluminum. The

low permeability seems to be due to the low hydrogen solubility and the passivity of the corresponding oxide formed on the chromium. No explanation can as yet be offered as to the location of magnesium in the sequence shown above. The position of copper in the order of hydrogen permeability was in agreement with that of solubility and diffusivity. It was very difficult to defect differences between the permeability of hydrogen in iron, nickel and cobalt because the corresponding solubilities and diffusivities are close one another. $LaNi_5$, Pt and Pd showed the greatest hydrogen for Pt is large although the solubility of hydrogen is low. The results obtained seem to give an indication of the "genuine" character of hydrogen permeation in various metals.

6. 4. Summary

An a-WO_3 film which is partially covered with an $LaNi_5$ film changed its body color when hydrogen was applied to the sample. The hydrogen permeability for various metals was examined by observing the developing of coloring of the a-WO_3 film with hydrogen permeated through the metal films on which an $LaNi_5$ was coated. The hydrogen permeability was in the following order; $LaNi_5$, Pt, Pd > Fe > Ni, Co, Ti > Mn > Cu > Mg, Cr > Al > Au, Ag, Zn.

Chapter 7

HYDROGEN SEPARATION USING RARE-EARTH HYDROGEN STORAGE ALLOY FILMS

7. 1. Introduction

Hydrogen separation has been studied using films of polymers, porous glasses, and metals[39]. A palladium film is known to exhibit excellent properties for hydrogen separation[40]. The film is , however, very expensive and must be operated at an elevated temperature. The use of a cheaper metal or an alloy instead of palladium would be advantageous for the hydrogen industries. $LaNi_5$ is considered to be a good candidate as a hydrogen separation material[41] because it is less expensive than Pd and has an admirable ability to absorb hydrogen at moderate temperatures and pressures. Some $LaNi_5$ films have been prepared by means of a flash-evaporation and of a sputtering method and have been investigated with respect to the hydrogen content in the films and mechanical properties. One of its most remarkable characteristics is that these films do not pulverize after more than 100 cycles of the hydrogen absorption-desorption process.

This finding led us to explore the possibility of

hydrogen separation using the films[42]. In the present study, the hydrogen separation characteristics of the films deposited on porous metal filters and polymer membranes were investigated.

7. 2. Experimental

7. 2. 1. Preparation of films

Metal substrates. Substrates were porous stainless steel discs of 3 mm thickness, 5 mm in diameter and 3 mm^2 effective surface area, which were made by sintering fine stainless steel particles(SUS 304, 0.5 μm in diameter), purchased from Shoketsu Kinzoku, Tokyo. These discs were washed first with acetone, 0.1 N-NaOH solution in order to defat, soaked in 0.1 N-HCl solution and finally rinsed with deionized water. The substrates were cleaned in an ultrasonic washing machine filled with methanol and then dried in the evacuated desiccator.

The deposition of $LaNi_5$ was performed by using the flash-evaporation. A distance between tungsten boat and the substrate was 40 mm and the substrate temperature was about 600 K. Before evaporating, the substrate was preheated for 60 second.

Cu was evaporated by using a conventional vacuum deposition method. As it was difficult to electroplate Ni on the stainless substrate directly, the substrate was coated with Cu before the Ni plating.

The Ni coating is made by depositing Ni electrolyt-

ically with a commercial electrolyte under following conditions: a temperature of 333 K, current densities of 5 A/dm^2(900 s)-7.5 A/dm^2(900 s)-10 A/dm^2(1800 s), Ni cathod.

For the Al plating, holes of the stainless filter were plugged with a molten Al in vacuo.

Polymer substrates. Substrates were two kinds of polymer membranes, Teflon(Toyofuron, 25 μm thick, Toray Co., Ltd.) and polyimide(Kapton, 40 μm thick, Toray-Du Pont Co., Ltd.). These substrates were cleaned in an ultrasonic washing machine filled with acetone.

The metal layers were deposited with an r.f. magnetron sputtering apparatus made by Daia Vacuum Engineering Co., Ltd., from an Ni or an $LaNi_5$ target. The substrate temperatures were in the range of 300-373 K. The $LaCo_5$ films were prepared by means of the flash-evaporating method.

7. 2. 2. Measurement of properties

Metal substrates. The sample obtained was inserted into the apparatus, as is shown in Fig. 1(a). Film activation was achieved by the following treatment. Initially a hydrogen admission-evacuation process was repeated several times at 363 K. Next a cycle in which the film temperature was lowered to a room temperature and raised to 363 K under an atmosphere of hydrogen was repeated several times.

An H_2-C_3H_8, H_2-CH_4, H_2-N_2 or H_2-Ar gas mixture was passed through the apparatus and then the resulting gas was collected in gas samplers at the outlet. Rates of permeation

of the gas through the film were measured and compositions of the resulting gas were analyzed using a Hitachi RMU-6E mass spectrometer.

Polymer substrates. A disc membrane 10 mm in diameter was inserted in a separation apparatus as is shown in Fig. 1(b). The stainless steel filter(Tokyo Seikoh Co., Ltd.) was used as a support for the film against the pressure.

An H_2(50 mol%)-Ar(50 mol%) gas mixture with a pressure of 1.5×10^5 Pa at 368 K was applied to the $LaNi_5$-deposited side of the membrane.

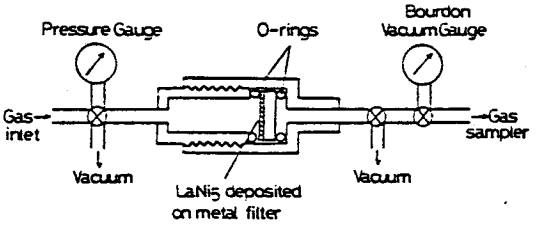

Fig. 1(a) Apparatus for investigating gas permeation.
- Metal filter -

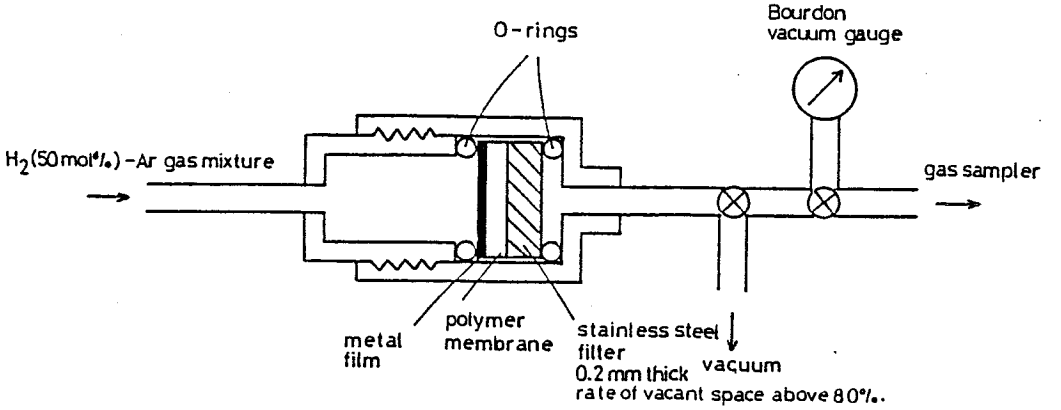

Fig. 1(b) Apparatus for investigating gas permeation.
- Polymer membrane -

7. 3. Results and Discussion

7. 3. 1. Structure of the films

Metal substrates. It is known that for a dilute solid solution of hydrogen in Ni or Al, hydrogen in the metals diffuses quickly[43,44]. Both Ni and Al easily plug the holes of the filter by the methods described in Section 7.2.1. and the strength of the Ni and Al layers obtained is larger than that of the $LaNi_5$ film. The metals, however, absorb hydrogen poorly compared with $LaNi_5$. Accordingly, it was thought that if the metals were coated with $LaNi_5$, hydrogen would permeate easily through the metals.

Figure 2(a) illustrates the structure of films used for the experiments. Film a is $LaNi_5$ directly deposited on the substrate. The thickness of the $LaNi_5$ film was 16.5 μm. For films b, c and d, copper was first deposited on the substrates(about 0.1 μm thick) in order to perform the nickel plating neatly, and then nickel was plated on them(about 50 μm thick). The nickel layer was employed to reinforece and to increase the durability of the film. Subsequently, $LaNi_5$ was deposited on the nickel layer. An advantage of these films is that this method can be carried out without a thick $LaNi_5$ film. Film d is film b further coated with about a

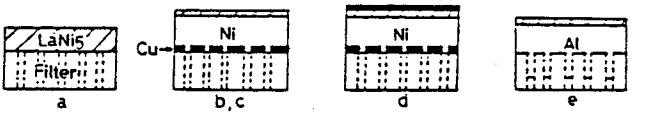

Fig. 2(a) Structures of the films.

- Metal filter -

0.1 μm thick copper film. In the case of film e, the stainless steel filter was first covered with an aluminum film and then with a 10^{-2} μm thick $LaNi_5$ film.

Pinholes or small cracks were ruled out in all films before hydrogen permeation because Ar did not pass through the films.

Polymer substrates. Figure 2(b) illustrates the structures of the films used for the experiments. Since the mechanical strength and the durability of the sputtered films were greater than those of the evaporated ones, the metal films were mainly prepared using the sputtering method.

Film b is an $LaNi_5$ film directly deposited on a Teflon or on a polyimide membrane. The thickness of the metal layer was 0.75 μm. For film d, nickel was first deposited on the substrates(0.73 μm, 1.23 μm, or 1.48 μm thick). The nickel layer was to reinforce the durability of the films. Subsequently, $LaNi_5$ was deposited on the nickel layer. Films a and c were for blank tests.

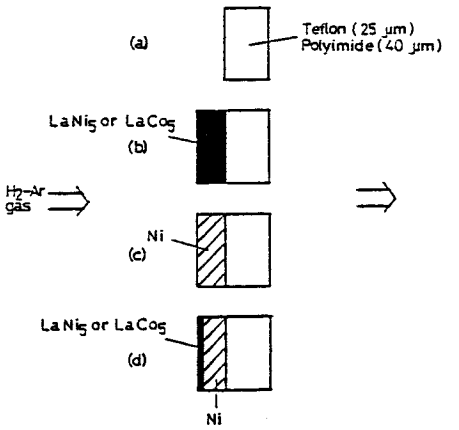

Fig. 2(b) Structures of the films.

- Polymer membrane -

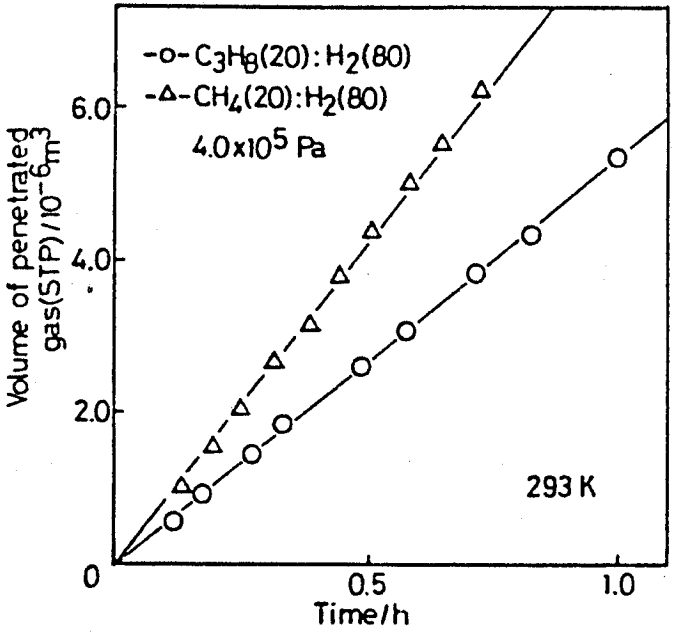

Fig. 3(a) Variation of the volume of permeated gas as a function of time. SM/$LaNi_5$(16.5 μm).

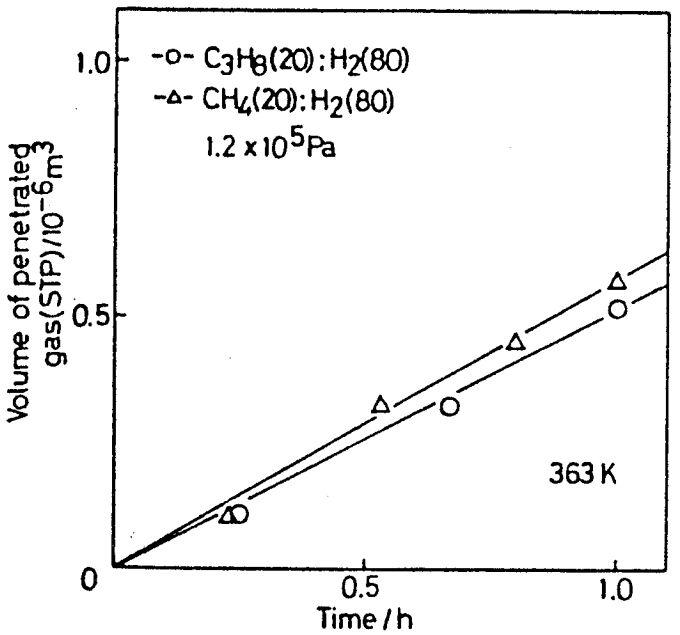

Fig. 3(b) Variation of the volume of permeated gas as a function of time. SM/Cu/Ni/$LaNi_5$(10^{-2} μm).

7. 3. 2. Performance characteristics of the films

Metal substrates. Figures 3(a) and 3(b) show the relationship between the amount of permeated gas and the time of gas sampling. A proportional relation between them indicates that the films were neither disintegrated by nor contaminated with the mixed gases applied.

The rates of permeation, the permeation coefficients and the hydrogen concentration in the penetrated gas for the films obtained are summarized in Table 1.

For film a, the hydrogen content after the treatment was very low. This is probably because very small cracks were developed when hydrogen was absorbed in the $LaNi_5$ film. This is also supported by the result of Fig. 3(a). The difference in the permeation rate between the two straight lines in the Figure seems to be because of the molecular-sieve effect for CH_4 and C_3H_8. The cracks, however, seem to disappear owing to desorption of hydrogen when the temperature of the film was increased because the gas flow then stopped. The cracks may be formed when hydrogen exists in the film.

As is shown in Table 1 the hydrogen concentration in the penetrated gas for film b is greater than that for film a. The difference in the gas composition applied does not affect the permeation rate.

The effect of the thickness of the $LaNi_5$ film on the rate of permeation and the hydrogen content in the penetrated gas was examined for 0.02 and 0.2 μm $LaNi_5$ films(Table 1, b, c). The permeation coefficient for the thinner $LaNi_5$

Table 1 Performance characteristics of $LaNi_5$ films

Film composition	*Gas composition* (mol.%)	*Primary pressure* (10^5 Pa)	*Temperature of film* (K)	*Rate of permeation* ($m^3 s^{-1}$)	*Permeation coefficient* ($m^2 s^{-1} Pa^{-\frac{1}{2}}$)[b]	*Hydrogen content after treatment* (mol.%)
a SM[a]/$LaNi_5$ (16.5 μm)	H_2 (80.0)-C_3H_8 (20.0)	4.0	293	13.39×10^{-10}	15.94×10^{-12}	80.9
	H_2 (80.0)-CH_4 (20.0)	4.0	293	24.23	26.85	80.4
b SM/Cu/Ni/$LaNi_5$ (0.02 μm)	H_2 (80.0)-N_2 (20.0)	1.2	363	1.44	8.38	89.7
	H_2 (80.0)-Ar(20.0)	1.2	363	1.58	9.06	83.1
c SM/Cu/Ni/$LaNi_5$ (0.20 μm)	H_2 (80.0)-C_3H_8 (20.0)	8.0	368	0.93	1.93	87.8
d SM/Cu/Ni/$LaNi_5$/Cu	H_2 (80.0)-C_3H_8 (20.0)	10.0	368	0.06	0.10	96.5
	H_2 (80.0)-CH_4 (20.0)	10.0	368	0.05	0.10	98.1
	H_2 (80.0)-N_2 (20.0)	10.0	368	0.05	0.07	95.3
	H_2 (80.0)-Ar(20.0)	10.0	368	0.05	0.10	94.5
e SM/Al/$LaNi_5$	H_2 (80.0)-C_3H_8 (20.0)	8.0	368	0.03	0.04	98.8
	H_2 (80.0)-CH_4 (20.0)	8.0	368	0.04	0.05	96.5

[a] Sintered metal filter.

[b] Units $m^3 mm^{-2} s^{-1} Pa^{-\frac{1}{2}}$ [8] derived from (volume of penetrated gas (STP))^3 × (thickness of the sample) × (surface area of the sample)$^{-2}$ × (time during permeation)$^{-1}$ × (difference of pressure)$^{-\frac{1}{2}}$.

film was about four times as large as that for the thicker one. Although $LaNi_5$ quickly absorbs hydrogen, the diffusion of hydrogen in the $LaNi_5$ hydride formed in the film is slow, so that the thinner $laNi_5$ film can be permeated by the gas more rapidly than the thicker one.

Film d gave an excellent value of hydrogen concentration in the permeated gas, though the permeation coefficient was very small.

An Al-coated sample(film e) instead of the Ni-coated sample shows the highest value of hydrogen concentration among the samples obtained. The reason why the rate of permeation for the film is so small seems to be that the molten Al soaks deeply into the channel of the filter.

Polymer substrates. Nickel films with various thicknesses deposited on the Teflon membranes were prepared, and the effects of the thickness of the metal layer on the hydrogen separation were studied. As is shown in Fig. 4, for a 0.5

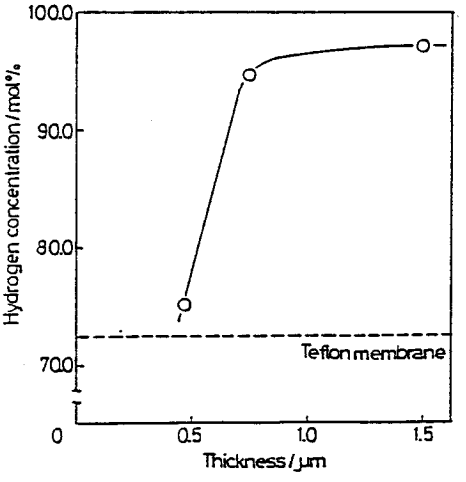

Fig. 4 Effects of thickness of nickel layer on hydrogen concentration in permeated gas.

μm-thick film the hydrogen concentration in the permeated gas was slightly larger than that for the Teflon-only membrane. It seems probable that most of the gas mixture passed through pinholes in the nickel film. However, for a 0.75 μm-thick film the hydrogen concentration increased remarkably. It can be considered that, above thickness of 0.75 μm, the Teflon membrane was almost completely covered with the nickel film and that the hydrogen applied permeated through the nickel layer.

Table 2 shows the hydrogen-separation ability of the $LaNi_5$ films deposited on the Teflon membrane. A gas of 50 mol% H_2 was found to be concentrated to 74.8 mol% by the use of the Teflon membrane alone. When the metal films were deposited on the Teflon, the hydrogen concentration incresed greatly. It was found that the permeation rate of the $LaNi_5$ film was several times as large as that of the Ni film, though the hydrogen concentration for the $LaNi_5$ film was slightly lower than that for the Ni film. There were no differences in characteristics for the permeation rate and the separation factor between the $LaNi_5$ film and the $Ni/LaNi_5$ multilayered film. The nickel film is able to permeate hydrogen easily because the thin $LaNi_5$ film coated on the nickel surface dissociates the hydrogen molecule easily and absorbs much hydrogen. Figure 5 shows the relationship between the permeation rate and the thickness of the metal layer and also the effects of the $LaNi_5$ layer on the hydrogen permeation of the Ni film. The permeation rate decreased with the increase in the thickness of the metal layer.

Table 2 Performance Characteristics of $LaNi_5$ and $LaCo_5$ films deposited on the Teflon membrane

Gas composition (mol%)	Film composition	Permeation rate (m^3s^{-1}) x10^{-12}	Permeability coefficient ($m^2s^{-1}Pa^{-1/2}$ [a]) x10^{-16}	Hydrogen content after treatment (mol%)	Separation factor
Ar(50)-H_2(50)	Teflon(T) (25μm)	43	2400	74.8	2.97
	0.75μm				
	T/$LaNi_5$	5.3	5.7	89.5	8.52
	T/Ni	0.99	1.1	94.7	17.9
	T/Ni/$LaNi_5$ (0.02μm)	5.4	6.3	91.9	11.3
	T/$LaCo_5$	<0.5	<0.5	75.2	3.03
	1.50μm				
	T/Ni	0.55	1.2	97.2	34.7
	T/Ni/$LaNi_5$ (0.02μm)	2.2	5.1	91.0	10.1
	1.31μm				
	T/Ni/$LaCo_5$ (0.08μm)	<0.5	< 1	83.1	4.92

Primary pressure: 1.5×10^5 Pa; temperature of film, 368 K,

a) Units $m^2s^{-1}Pa^{-1/2}$ is derived from (volume of permeated gas(STP))x (thickness of the sample)x(surface area of the sample)$^{-1}$x(the time required for permeation)$^{-1}$x(difference in pressure)$^{-1}$.

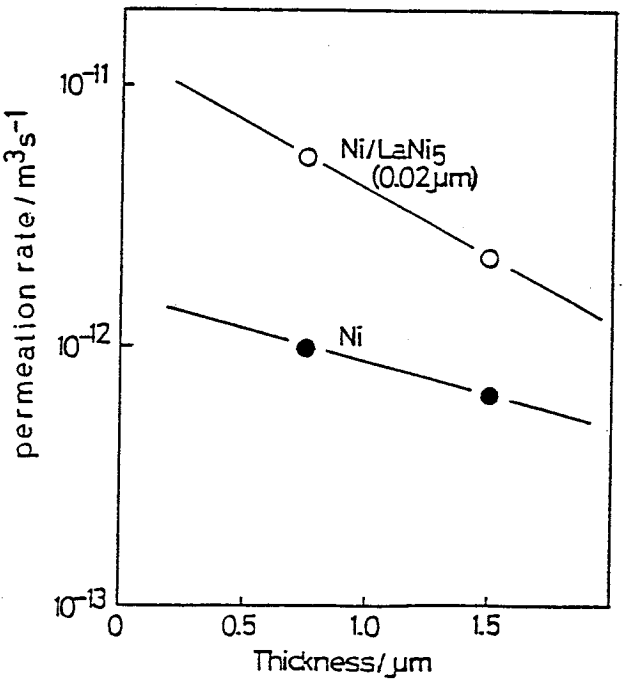

Fig. 5 Relationship between permeation rate and thickness of metal layer.

Also, for the 1.5 μm-thick film, the permeation rate for the $Ni/LaNi_5$ multilayered film was much larger than that for the Ni film.

Table 3 shows the hydrogen separation characteristics of the $LaNi_5$ film deposited on the polyimide membrane. The polyimide membrane itself exhibited a high hydrogen-separation factor. The highest separation factor was obtained for the $Ni/LaNi_5$ multilayered film. The reason why the separation capability of the $Ni/LaNi_5$ film is excellent seems to be that the adhesion between the polyimide membrane and the metal film was superior to that between the Teflon membrane and the metal film.

An $LaCo_5$ film is not suited for the hydrogen separator because the mass of the permeated gas obtained from the films deposited on both the Teflon and polyimide membranes was extremely small and these separation factors were not so good(Table 2 and 3). This seems to be caused by the small hydrogen concentration in the $LaCo_5$ film[45].

Table 3 Performance characteristics of $LaNi_5$ and $LaCo_5$ films deposited on the polyimide membrane

Gas composition (mol%)	Film composition	Permeation rate (m^3s^{-1}) x10^{-12}	Permeability coefficient ($m^2s^{-1}Pa^{-1/2}$) x10^{-16}	Hydrogen content after treatment (mol%)	Separation factor
Ar(50)-H_2(50)	Polyimide(I) (40μm)	3.1	188	95.2	19.8
	1.25μm				
	I/Ni	2.1	3.8	96.6	28.4
	I/Ni/$LaNi_5$ (0.02μm)	2.7	5.0	97.6	40.7
	1.31μm				
	I/Ni/$LaCo_5$ (0.08μm)	<0.5	< 1	95.1	19.4

Primary pressure: 1.5x10^5 Pa; temperature of film, 368 K.

In Table 4, the characteristics of the $LaNi_5$ film using the polymer as a substrate for the hydrogen separation are compared with those of the $LaNi_5$ film deposited on a porous stainless steel filter as well as those of a Pd film [40,46]. As for the thickness of the metal layer, high-purity hydrogen gas was obtained with an $LaNi_5$ film only 1 μm thickness for the polymer-substrate sample. The permeation rate for the $LaNi_5$ film coated on the polymer is very low, but this is not a serious problem, because for the polymer membrane it is easy to increase the area of the gas contact surface. For instance, if a hollow fiber on which the metal layer is formed is bundled, a large surface area can be obtained.

The $LaNi_5$ films deposited on the nickel-coated polymer substrate or the metal filter are relatively cheap and easy to prepare.

Table 4 Estimation of $LaNi_5$ films deposited on the metal filter and the polymer membrane for hydrogen separation

	Thickness of the metal layer (μm)	Permeation rate	Hydrogen-separation factor
Pd	100~200	1	Above 66
Metal filter substrate	50	$1/10^2$	2.25~20.6
Polymer substrate	1	$1/10^3$	10~40

7. 4. Summary

The hydrogen-separation ability of $LaNi_5$ films deposited on a nickel or aluminum coated porous stainless steel filter was investigated. A gas mixture(80 mol% H_2) was applied to the films. The composition of the resulting gas was 83 98 mol% H_2 for the Ni/$LaNi_5$ film, and was 96 99 mol% H_2 for the Al/$LaNi_5$ film, respectively. Polymer membranes were also used as a substrate. Hydrogen was concentrated from 50 mol% to 97.6 mol%. The permeation rate of the Ni/$LaNi_5$ film was found to be larger than that of the Ni film because the thin $LaNi_5$ film coated on the nickel surface dissociates the hydrogen molecule easily and absorbs much hydrogen.

Chapter 8

CONCLUDING REMARKS

In this thesis, preparation of thin films of hydrogen storage alloys and properties of the films, such as mechanical and electrical properties, and hydrogen contents in the films were described, and the mechanism of hydrogen absorption-desorption was considered. In addition, a prototype of new hydrogen separation technique using the films was proposed. Main results of this work are as follows.

1. Thin films of $LaNi_5$, $SmCo_5$ and $LaCo_5$ were prepared using a flash evaporation-deposition or a sputtering method. The films obtaimed were amorphous, and were found not to pulverize after repeated hydrogenation-dehydrogenation cycles. The density of the sputtered $LaNi_5$ film was about 6 gcm^{-3}, which was larger than that of the deposited film or smaller than that of a crystalline sample. Thermal conductivities of the films were larger than those of bulk samples.

2. Mechanical properties of the sputtered $LaNi_5$ films deposited on various substrates were measured after 100 cycles of hydrogen absorption-desorption process, which were the maximum cycle number appled for this film. The result was in the following order for the substrates used, Ni foil>Ni>Al foil >Cu foil>Cu>Al>glass. The deposited film on a copper foil or an aluminum foil has not been disintegrated.

3. Electrical resistivity measurements for the deposited films were performed under hydrogen atmospheres. Resistivities initially increased and then maintained a constant value or decreased during the hydrogen absorption process. As for the desorption process, the reverse phenomena were observed.

The formation mechanism of hydrogen anions-conduction electrons was used to explain the mechanism of hydrogenation for the rare-earth alloys. The resistivity changes suggest that the following steps take place during hydrogen absorption. The dissociated hydrogen atoms take on the conduction electrons of the metals and become the hydrogen anions. The number of electrons in the conduction band of the metals decreases, and consequently the resistivity increases, followed by the occurrence of the formation of a high conductivity hydride.

The second explanation for the resistivity change on hydrogenation is that the band structure itself may be changed.

4. The hydrogen content in the films obtained was found to be smaller than that in crystalline samples. The hydrogen concentration in the $LaNi_5$ films was much larger than that in the $LaCo_5$ films. In pressure-composition isotherms, the hydrogen concentration increased monotonously with pressure despite the variations both in temperature and in film thickness suggesting that the single phase which dissolves hydrogen anions seems to be predominant.

5. An a-WO_3 film which is partially covered with an $LaNi_5$ film changed its body color when hydrogen was applied to the sample. The hydrogen permeability for various metals was examined by observing the developing of coloring of the a-WO_3 film with hydrogen permeated through the metal films on which an $LaNi_5$ was coated. The hydrogen permeability was in the following order; $LaNi_5$, Pt, Pd > Fe > Ni, Co, Ti > Mn > Cu > Mg, Cr > Al > Au, Ag, Zn.

6. The hydrogen-separation ability of $LaNi_5$ films deposited on a nickel or aluminum coated porous stainless steel filter was investigated. A gas mixture(80 mol% H_2) was applied to the films. The composition of the resulting gas was 83 98 mol% H_2 for the Ni/$LaNi_5$ film, and was 96 99 mol% H_2 for the Al/$LaNi_5$ film, respectively. Polymer membranes were also used as a substrate. Hydrogen was concentrated from 50 mol% to 97.6 mol%. The permeation rate of the Ni/$LaNi_5$ film was found to be larger than that of the Ni film because the thin $LaNi_5$ film coated on the nickel surface dissociates the hydrogen molecule easily and absorbs much hydrogen.

ACKNOWLEDGEMENT

The author is greatly indebted to Professor Jiro Shiokawa at the Department of Applied Chemistry, Faculty of Engineering, Osaka University for his continuous guidance and encouragement throughout this work.

The author is also indebted to Professor Hiroshi Yoneyama for his kind suggestions in the course of this thesis.

The author is deeply grateful to Professor Toshio Tanaka for his constant guidance and warmhearted encouragements.

The author wishes to express his sincere thanks to Associate Professor Gin-ya Adachi for his significant direction during the course of the study, for his kind discussion in the preparation of the manuscript, and for his tender suggestions to my private life.

It is a great pleasure to express his hearty thanks to Professor Jyun-ichi Kobayashi, Shizuoka University for his intimate guidance and helpful advices.

The author would like to acknowledge Dr. Yoshiyuki Hirashima, Dr. Tsuyoshi Arakawa, Dr. Tsutomu Shin-ike, Associate Professor Hiroshi Nagai, Dr. Mineo Sato, Dr. Ken-ichi Machida, Dr. Hiroshi Ishikawa, Dr. Tetsuo Sakai, and Dr. Kenji Ishikawa for their significant discussion, and Dr. Nobuhito Imanaka for his helpful advise and heartful encouragement.

Thanks are given to the author's co-workers, Mr. Noboru Taniguchi, Mr. Atsushi Hori, Mr. Yasuyuki Yagi, Mr. Toshiyuki Shimogohri, and Mr. Hajime Seri for their assistance, and Mr. Ken-ichi Niki, Mr. Hiroshi Nagai, Mrs. Ichiko Kawamoto, Mrs. Maki Kitora, Miss. Harumi Wada, Mr. Kouji Sakai, Mr. Jyunji Kawafuku, Mr. Hiroshi Kurachi, Miss. Yumi Kawahara, Mr. Hiroyuki Fujikawa, Mr. Shigeharu Matsubayashi, Mr. Yasuo Yamaguchi, Mr. Yoshikazu Tsunemine, Mr. Hirofumi Nakamura, Mr. Hisao Imai and all the other members of Shiokawa group for their help and valuable suggestions.

Finally, The author greatfully acknowledges the hearty encouragement and assistance given by his father, Professor Masakazu Sakaguchi, his mother, Setsuko Sakaguchi, his elder sister, Reimi Ohkubo, and his younger sister Miki Sakaguchi.

References

(1) K. H. J. Buschow and H. H. van Mal, J. Less-Common Met., 29(1972)203.

(2) H. H. van Mal, K. H. J. Buschow and A. R. Miedema, ibid., 35(1974)65.

(3) J. H. N. van Vucht, F. A. Kuijpers and H. C. A. M. Bruning, Philips Res. Rept., 25(1970)133.

(4) D. P. Gregory, "The Rare Earths in Modern Science and Technology," ed by G. J. McCarthy and J. J. Rhyne, Plenum Press New York, 1977, pp. 1.

(5) W. E. Wallace, R. F. Karllcek, Jr., and H. Imamura, J. Phys. Chem., 83(1979)1708.

(6) R. L. Cohen and J. H. Wernick, Science, 214(1981)1081.

(7) S. Ono and Y. Osumi, Seramikkusu, 14(1979)339.

(8) Y. Osumi, Kagaku, 36(1981)145.

(9) R. Wang, Mater. Res. Bull., 11(1976)281.

(10) L. Belkbir, E. Joly, N. Gerard, J. C. Achard and A. Percheron-Guegan, J. Less-Common Met., 73(1980)69.

(11) L. Schlapbach, A. Seiler, F. Slucki and H. C. Siegmann, J. Less-Common Met., 73(1980)145.

(12) G. Adachi, K. Niki and J. Shiokawa, J. Less-Common Met., 81(1981)345.

(13) G. Adachi, K. Niki, H. Nagai and J. Shiokawa, ibid., 88(1982)213.

(14) H. Ishikawa, T. Sakai, K. Oguro, N. Taniguchi, H. Sakaguchi, G. Adachi and J. Shiokawa, 4th Meeting of the Rare Earth Society of Japan, Kyoto, March 1986, Abstr., No. 1A01.

(15) N. Taniguchi, H. Sakaguchi, G. Adachi, J. Shiokawa, H. Ishikawa, T. Sakai and K. Oguro, 52nd National Meeting of the Chemical Society of Japan, Kyoto, April 1986, Abstr., No. 1M08.

(16) J. H. Wernich, S. Geller, Acta Crystallogr., 12(1959) (1959)662.

(17) H. Sakaguchi, N. Taniguchi, H. Nagai, K. Niki, G. Adachi and J. Shiokawa, J. Phys. Chem., 89(1985)5550.

(18) L. A. Haluska, Am. Soc. Test Mater. Spec. Tech. Publ. 769(1982)16.

(19) B. N. Chapman, J. Vac. Sci. Technol., 11(1974)106.

(20) Kagaku Binran, 3rd edn., Kiso Hen, The Chemical Society of Japan, Maruzen Inc., 1984, p.21.

(21) Ibid., p.502.

(22) K. Ramakrishna and O. N. Srivastava, J. Mat. Sci. Lett., 6(1987)15.

(23) H. Kitada, Nippon Kinzoku Gakkaishi, 41(1977)412.

(24) R. V. Bucur and T. B. Flanagan, Z. Phys. Chem.(Frankfurt am Main), 88(1982)213.

(25) G. A. Frazier and R. Glosser, J. Less-Common Met., 74(1980) 89.

(26) F. H. M. Spit, J. W. Drijver and S. Z. Radelaar, Z. Phys. Chem.(Frankfurt an Main), 74(1980)279.

(27) K. Suzuki, J. Less-Common Met., 89(1983)183.

(28) K. Nakamura, Scr. Metall., 18(1984)793.

(29) G. G. Libowitz and A. J. Mealand, J. Less-Common Met., 101(1984)131.

(30) R. Feensta, G. J. de Bruin-Hordijk, H. L. M. Bakker, R. Griessen and D. G. de Groot, J. Phys. F, 13(1983) L13.

(31) A. Denda, A. Takano, T. Okada, T. Ebisawa, H. Uchida, 100th National Meeting of The Japan Institute of Metals, Tokyo, April 1987, Abstr., No. 600.

(32) S. K. Deb, Phil. Mag. 22(1973)801.

(33) J. V. Gabrusenoks, P. D. Cikmach, A. R. Lusis, J. J. Kleperis and G. M. Ramans, Solid State Ionics, 14 (1984)25.

(34) J. J. Kleperis, P. D. Cikmach and A. R. Lusis, Phys. Stat. Sol.(a) 183L(1984)291.

(35) G. Adachi, H. Sakaguchi, T. Shimogohri and J. Shiokawa, J. Less-Common Met., 116(1986)L13.

(36) N. A. Galaktionova, "Kinzoku nai no Suiso". ed by K. Endo, Ni-Sso Tsuushin Sha, Wakayama(1967).

(37) Y. Fukai, Nippon Kinzoku Gakkai Kaiho, 24(9)(1985)707.

(38) Kagaku Binran, 3rd edn., Kiso Hen I, The Chemical Society of Japan, Marusen Inc., 1984, p.22.

(39) T. Sakai, H. Ishikawa, N. Wakabayashi, K. Oguro and E. Ishii, Osaka Kohgyo Shikenjyo kaihoh, 35(4)(1984)60.

(40) Y. Osumi, Soda to Enso, 11(1984)446.

(41) T. Gamo, Y. Moriwaki, N. Yanagihara and T. Iwaki, J. Less-Common Met., 89(1983)495.

(42) G. Adachi, H. Nagai and J. Shiokawa, ibid., 97(1984)L9.

(43) G. Euringer, Zeir. Phys., 37(1)(1935)96.

(44) A. Chang and M. Bennett, J. Iron and Steel Inst., 170 (1952)205.

(45) H. Sakaguchi, Y. Yagi, N. Taniguchi, G. Adachi and J. Shiokawa, ibid., 135(1987)137.

(46) N. Taguma, M. Tada and T. C. Huang, Proceedings of the Faculty of Engineering, Tokai University, 1(1969)53.